Performance Analysis of Super-Twisting Sliding Mode Controller for Aircraft Pitch Control

Mulualem Geleta Gebeyehu

A Thesis Submitted to

The Department of Electrical Power and Control Engineering School of Electrical Engineering and Computing

Presented in Partial Fulfillment of the Requirement for the Degree of Master's in Electrical Power and Control Engineering (Control Engineering)

Office of Graduate Studies

Adama Science and Technology University

Mar, 2023

Adama, Ethiopia

Performance Analysis of Super-Twisting Sliding Mode Controller for Aircraft Pitch Control

Mulualem Geleta

Advisor: Prof. Gang Gyoo Jin

A Thesis Submitted to

The Department of Electrical Power and Control Engineering School of Electrical Engineering and Computing

Presented in Partial Fulfillment of the Requirement for the Degree of Master's in Electrical Power and Control Engineering (Control Engineering)

Office of Graduate Studies

Adama Science and Technology University

Mar, 2023

Adama, Ethiopia

DECLARATION

I hereby declare that this Master Thesis entitled "Performance analysis of Super-Twisting Sliding Mode Controller for Aircraft Pitch Control" is my original work. That is, it has not been submitted for the award of any academic degree, diploma or certificate in any other university. All sources of materials that are used for this thesis have been duly acknowledged through citation.

Mulualem Geleta Gebeyehu ______ ____________________ _____________

Name of the student Signature Date

RECOMMENDATION

I, the advisors of this thesis, hereby certify that we have read the revised version of the thesis entitled "Performance analysis of Super-Twisting Sliding Mode Controller for Aircraft Pitch Control" prepared under our guidance by **Mulualem Geleta Gebeyehu** submitted in partial fulfillment of the requirements for the degree of Mater's of Science in Control Engineering. Therefore, I recommend the submission of revised version of the thesis to the department following the applicable procedures.

Prof. Gang Gyoo Jin	____________________	________________
Advisor	Signature	Date

APPROVAL SHEET

I, the advisors of the thesis entitled "Performance analysis of Super-Twisting Sliding Mode Controller for Aircraft Pitch Control" and developed by Mulualem Geleta Gebeyehu, hereby certify that the recommendation and suggestions made by the board of examiners are appropriately incorporated into the final version of the thesis.

Prof. Gang Gyoo Jin		
Advisor	Signature	Date

We, the undersigned, members of the Board of Examiners of the thesis by Mulualem Geleta Gebeyehu have read and evaluated the thesis entitled "Performance analysis of Super-Twisting Sliding Mode Controller for Aircraft Pitch Control" and examined the candidate during open defense. This is, therefore, to certify that the thesis is accepted for partial fulfillment of the requirement of the degree of Master of Science in Control Engineering.

Chairperson	Signature	Date
Internal Examiner	Signature	Date
Dr Beteley Teka (PhD)		30-03-2023
External Examiner	Signature	Date

Finally, approval and acceptance of the thesis are contingent upon submission of its final copy to the Office of Postgraduate Studies (OPGS) through the Department Graduate Council (DGC) and School Graduate Committee (SGC).

Department Head	Signature	Date
School Dean	Signature	Date
Office of Postgraduate Studies, Dean	Signature	Date

ACKNOWLEDGEMENTS

First and foremost, I would like to thank the Almighty God for protecting me and bless his loving heart for giving us St. Mary as our Mother, who gives me the strength to finish this thesis work.

I would also like to thank and appreciate my advisor, Professor Gang Gyoo Jin, for his heartfelt support and guidance. He has given me nice guidance, inspiration and suggestions throughout doing this thesis work.

Furthermore, I really would like to thank Yeabisra Wubishet, Kiflemariam Abay and Habtamu Minale for their valuable advises willingness to share their knowledge, and numerous suggestions on all aspects of documentation preparation and writing.

Finally, I want to express my gratitude to my family members and friends for their support and all of their previous sacrifices.

TABLE OF CONTENTS

LIST OF TABLES

LIST OF FIGURES

LIST OF ACRONYMS

CG	Center of Gravity
IAE	Integral Absolute Error
IAEU	Integral Absolute Error and Control signal
ISE	Integral of Square Error
ITAE	Integral of time Multiplied Absolute Error
MATLAB	Matrix Laboratory
PID	Proportional Integral Derivative
PSO	Particle Swarm Optimization
QFT	Quantitative Feedback Theory
SMC	Sliding Mode Control
STSMC	Super Twisting Sliding Mode Control
VSS	Variable Structure Control
ZN	Zeigler Nichols

ABSTRACT

Because it was adjusted manually in the early days of aviation, maintaining an aircraft's pitch at the appropriate degree required constant pilot attention. The effectiveness of the aircraft system depends on a well-designed tracking controller to stabilize the aircraft pitch and follow the intended reference signal because the aircraft system is a highly nonlinear and unstable system. The performance analysis of STSMC, which is employed for tracking control of aircraft pitch with dynamic pressure change and external disturbance, is the main emphasis of this research work. The SMC controller is also used for comparisons. By employing the PSO algorithm to minimize the IAEU, the proposed STSMC controller parameters are produced. Both controllers' tracking capabilities using various reference signals are tested using MATLAB software, as well as the durability of their performance when subjected to dynamic pressure change and external disturbance force. By lowering the settling time, rise time, and peak time by 76.72%, 77.40%, and 65.35%, respectively, the obtained simulation results show that the STSMC approach beats the SMC. Similar to this, by reducing the IAEU value for both multiple step signals and ramp signals, the STSMC retains superior tracking performance. Both controllers' performance resilience is evaluated utilizing dynamic pressure fluctuations of up to 10% increment and an outside disturbance force. The suggested STSMC control approach yields peak times, rise times, and settling times in the 10% increment of dynamic pressure of 0.1750sec, 0.0877sec, and 0.1073sec, respectively. These times are small in compared to the SMC. The STSMC provides 0.1620sec, 0.0785sec, and 0.0951sec of peak, rising, and settling times during the external disturbance force rejection test. The STSMC provides 0.4314sec, 0.1879sec, and 0.6145sec of peak time, rise time, and settling time, respectively, which are all minimal compared to the SMC, for the tracking performance robustness against both dynamic pressure fluctuations and external disturbance force. The simulation outcomes generally demonstrated that the proposed STSMC outperformed the SMC controller in terms of tracking performance and robustness against dynamic pressure variation and external disturbance force.

Key Words: *STSMC, SMC, Aircraft, Particle swarm optimization.*

CHAPTER ONE

INTRODUCTION

1.1 Background

Aircraft technology has revolutionized human life by allowing people and goods to be transported regionally and internationally. Aviation has significantly reduced travel time and cost while also revolutionizing the travel experience with the introduction of in-flight luxuries not commonly available in other modes of transportation such as ground vehicles, trains, or boats (Wahid et al., 2010).

The flying qualities of an aircraft are required and essential for a safe flight envelope. The airplane's poor flying qualities will make it difficult to fly and potentially dangerous in all conditions, including climb, cruise, and approach phase. The primary goal of an aircraft automatic control system is to keep passengers and crew members safe. This is accomplished by analyzing the aircraft's dynamic performance, such as flight stability analysis and the automatic flight control system (Johari et al., 2018).

The designs of modern high performance aircraft are unstable to rise their facile and enable them to perform quarrel maneuver. Control of such aircraft needs constant follow up of pilot which enables the pilot to tiredness. Therefore automatic control system or autopilot is important. The pilot gets assistance from autopilot when performing tasks such as maintaining a specific orientation, altitude and orientation. It can also give assistance when performing tasks beyond human capabilities such as landing in bad weather or poor visibility condition. In general, the role of automatic controllers in modern aircraft design is expressed in terms of reducing the complexity of manual handling and improving system efficiency (Hamid & Babar, 2019).

An aircraft has a fixed wing that is propelled by an engine and can rotate in roll, pitch, and yaw. Because of the complicated dynamics of the aircraft, designing a control system is a difficult task. Furthermore, proper aircraft maneuvering is difficult because an aircraft's motion is highly coupled.

The design of the flight control system is a nonlinear control problem due to the changes in an aircraft's dynamics with flight conditions and aircraft configuration. As a result, a stable and adequately damped dynamic model in one flight condition may become unstable or at least adequately damped in another. To overcome such a problem, the aircraft requires a highly designed nonlinear control system that provides adequate control in a variety of flight conditions (Chrif et al., 2015).

Any flight will cause an aircraft to rotate about a point known as the center of gravity, which represents the average location of the aircraft's mass (CG). Each of the axes of the three-dimensional coordinate system defined by the center of gravity is perpendicular to the other two axes. The orientation of an aircraft can be defined by the amount of rotation of the parts of the aircraft along this principal axis. The pitch axis is perpendicular to the aircraft's centerline and lies in the plane's wings. An aircraft's nose can move up or down in a pitch action.

The dynamics of an aircraft are highly nonlinear, with many uncertainties and parameter variation. In addition, untraceable variation occurs in its operating environment. In this research work, rigid body aircraft are considered and assumed to fly at constant altitude and velocity. The motion of an aircraft consists of three rotational and three translational motions, as well as six degrees of freedom. Six nonlinear coupled differential equations serve as its mathematical representation. The aerodynamic forces and moments acting at an aircraft's center of mass are used to drive the equation of motion based on Newton's law of motion (Radhakrishnan & Swarup, 2020).

The position and orientation of an aircraft are expressed in a fixed coordinate system relative to the body. The coordinate system is three-dimensional, with x-y-z axes that are mutually perpendicular to each other and an origin that coincides with the aircraft's center of mass, as shown in Figure 1.1. The three rotational motions of these axes are roll, pitch, and yaw. Roll is rotation about the longitudinal axis (x), yaw is rotation about the vertical axis (z), and pitch is rotation about the lateral axis (y) (Radhakrishnan, 2020).

The primary control surfaces on an aircraft are the ailerons, rudder, and elevators. Ailerons on the wing's outer rear edge control roll. Rudder controls yaw on the vertical tail fin, and elevators control pitch on the horizontal tail surface (Radhakrishnan, 2020).

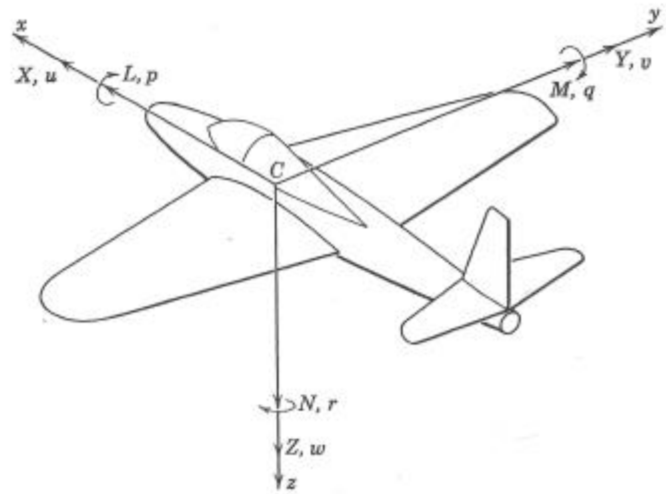

Figure 1.1 Aircraft body fixed coordinate system (Radhakrishnan, 2020).

The aircraft equation of motion is made up of six nonlinear equations that are decoupled into sets known as longitudinal and lateral equations of motion. In the vertical plane, the longitudinal equation of motion consists of pitching and translation. Rolling, side slipping, and yawing are all components of the lateral equation of motion (Radhakrishnan, 2020). As a result, only the longitudinal equation of motion is taken into consideration in this research work for pitch control.

The resulting response of an aircraft to applied forces and moments is described by a set of equations, which is referred to as the equation of motion. The aircraft is subjected to gravitational, thrust, and aerodynamic forces. Gravitational forces act through CG, resulting in a zero moment about CG (Shaji, 2015).

The elevator in the longitudinal plane controls the pitch of an aircraft. When the elevator control is moved backwards, the rear of the elevator deflects upwards and the tail is given negative camber, resulting in downward forces that imply the tail pitching down and the plane pitching up. Similarly, as the elevator moves forward, the rear of the elevator deflects downwards and the tail is given positive camber, resulting in an upward force that affects the tail's pitch up and the airplane's pitch down. This research paper focuses on the design of an autopilot that controls an aircraft's pitch in order to reduce the workload of the flight crew during the cruising stage.

Several techniques and algorithms have been proposed by various researchers for controlling aircraft pitch control. Some of these include dynamic inversion and PID controller, observer state feedback, quantitative feedback theory, fuzzy PID, SMC techniques, and adaptive controller that use linearized equations of motion to control an aircraft's pitch.

This research work presents the design of an autopilot that controls the pitch of an aircraft using a Super-Twisting sliding mode controller. The pitch is controlled by the SMC controller. The higher order SMC is added to the pure SMC to avoid the chattering problem caused by the frequency of oscillation. Both conventional SMC and STSMC control parameters are tuned by PSO algorithm. The overall system was mathematically designed and implemented using the MATLAB/Simulink software tool. Finally, the performance of the sliding mode and super-twisting sliding mode controllers is compared.

1.2 Statement of the Problem

An airplane is a sizable, complex item of mechatronic technology that has several uses. Longitudinal and lateral controls are components of the aircraft control system. The elevator controls the aircraft's pitch motion under longitudinal control. Both during the takeoff phase and throughout steady flight, the aircraft's pitch control must shift. Because it was adjusted manually in the early days of aviation, maintaining an aircraft's pitch at the appropriate degree required constant pilot attention. As a result, the sustained focus of a pilot during long flights may cause considerable weariness. Hence an autopilot pitch controller should be installed in that aircraft. And the coupling of modeling mistakes, nonlinear dynamics, and parameter changes that define an aircraft and its operational environment are the main problems with aircraft pitch control systems. However, it can be challenging to control a nonlinear flight. The modeling of uncertainties and parameter variations that describe the aircraft's characteristics are the major challenges in designing a nonlinear flight control system. As a result, the aircraft should be controlled by the appropriate control systems. The aircraft must be stabilized and many critical parts of the aircraft must be controlled without difficulty. The most critical parts are the elevator for pitch, rudder for yaw, and aileron for roll motion movement. Most previously designed controllers for an aircraft are linear controllers for linear systems, and they work only to minimize the system's transient response while ignoring robustness to parameter variation and external disturbance. Sliding mode controller is a robust controller with chattering, so it requires another controller to overcome this chattering and efficiently control the pitch of the aircraft. The super twisting sliding mode controller is a robust and it also overcomes the chattering problem of sliding mode controller.

1.3 Objectives

1.3.1 General Objective

The general objective of this thesis is the performance analysis of super-twisting sliding mode controller (STSMC) to control the pitch of an aircraft.

1.3.2 Specific Objectives

- To develop an equivalent mathematical model of an aircraft longitudinal component.
- To test stability of the SMC control system using Lyapunov stability theorem.
- To apply super-twisting techniques to eliminate chattering phenomena of the sliding mode controller.
- To tune the SMC and STSMC controller parameter optimally using PSO algorithm.
- To compare the performance results of the STSMC and SMC controller from simulation works.
- To test performance robustness by considering dynamic pressure variation and external disturbance force.

1.4 Scope of the Study

The thesis focuses on the mathematical modeling and simulation design of aircraft motion control, as well as the design of a super-twisting sliding mode controller for pitch control. MATLB/Simulink is used to simulate a super-twisting sliding mode controller for aircraft pitch control. Finally, the controller's performance is evaluated and discussed.

1.5 Limitation of the Study

The scope of the research is limited to simulating the system with MATLAB/Simulink and demonstrating how the system's various components interact with one another. This is due to the difficulty in obtaining the components required for actual system implementation. It also necessitates the additional time and money spent on developing the actual prototype implementation.

1.6 Motivation of the Study

An aircraft provides necessary local, regional, and international connectivity and makes it simpler to engage in the global economy. It facilitates trade, encourages tourism, and produces job opportunities. The aircraft's pitch movement is essential for ensuring the inherent safety of the crew and passengers as well as maximum stability of the aircraft. So, this research work concentrated on aircraft pitch control.

1.7 Significance of the Study

This research work describes the design of an autopilot that controls the aircraft's pitch using a super-twisting sliding mode controller. The findings of this study will have the following significance.

- It reduces the workload of the flight crew while cruising and assists them in landing the plane in bad weather.
- The pitch control of aircraft systems controlled by STSMC is robust to parameter variation (dynamic pressure) and external disturbances (wind dust).

- It improves tracking performance of the aircraft pitch by decreasing the system transient characteristics such as settling time, rise time and peak time.

1.8 Thesis Organization

This thesis is organized into five chapters.

Chapter 1: The first chapter includes introduction of the research work, statement of the problems, objectives, significance, scope, and limitation of the research, methodology and definition of terms.

Chapter 2: Presents a literature review on the background of aircraft pitch control, different control mechanisms, and working of aircraft system are discussed.

Chapter 3: Covers mathematical modeling of an aircraft and

Chapter 4: The controller designs for an aircraft pitch control.

Chapter 5: Summarizes the results of the simulation work and discusses them.

Chapter 6: Finally, conclusion and recommendation are made.

CHAPTER TWO

LITERATURE REVIEW

2.1 Chapter Overview

The two major sections are covered in detail in this chapter. An overview of the aircraft system, including forces operating on it, the aircraft's axis, and the flight control system is given in the first section. The second portion is a study of earlier relevant works on the proposed system's control utilizing different controllers, along with those works' advantages and disadvantages.

2.2 Theoretical Background

2.2.1 Forces Acting on the Aircraft

During flight, all aircraft are affected by the forces of thrust, drag, lift, and weight. The basic concepts in flight control systems are the working principle of these forces and how to control them. In a level flight, the sum of these opposing forces is zero (John, 2016).

Thrust causes an aircraft to move in the direction of motion. It is produced by a propeller or a jet engine. An aircraft cannot move unless the thrust force is greater than the drag force. The aircraft keeps moving and changing speeds until thrust and drag are equal. The thrust and drag forces must be equal for the aircraft to move at a constant air speed. Level flight may occur at various speeds. Angle of attack and thrust must be coordinated to keep the aircraft level in flight at different speeds (John, 2016).

Lift force is the force that keeps an aircraft in the air. The wings of an aircraft produce the majority of its lift. Lift force is created when an object moves through air. Fluid and motion are important in generating lift force. The dynamic effect of moving air over the wing produces lift force. Lift opposes the weight's downward force.

Drag is a force that opposes the motion of an aircraft through the air. Drag is classified into two types: parasite drag and induced drag. Site drag is caused by the shape of the aircraft, as well as the smoothness or roughness of the aircraft's surface. The effect on the production of lift causes induced drag (John, 2016).

Weight is the force created by the earth's gravitational attraction on the aircraft. The weight of an aircraft is always directed towards the center of the earth. Gravitational force is represented by weight.

The pilot must understand the effects of thrust, drag, lift, and weight on the aircraft during continuous flight and how to control the balance of these forces.

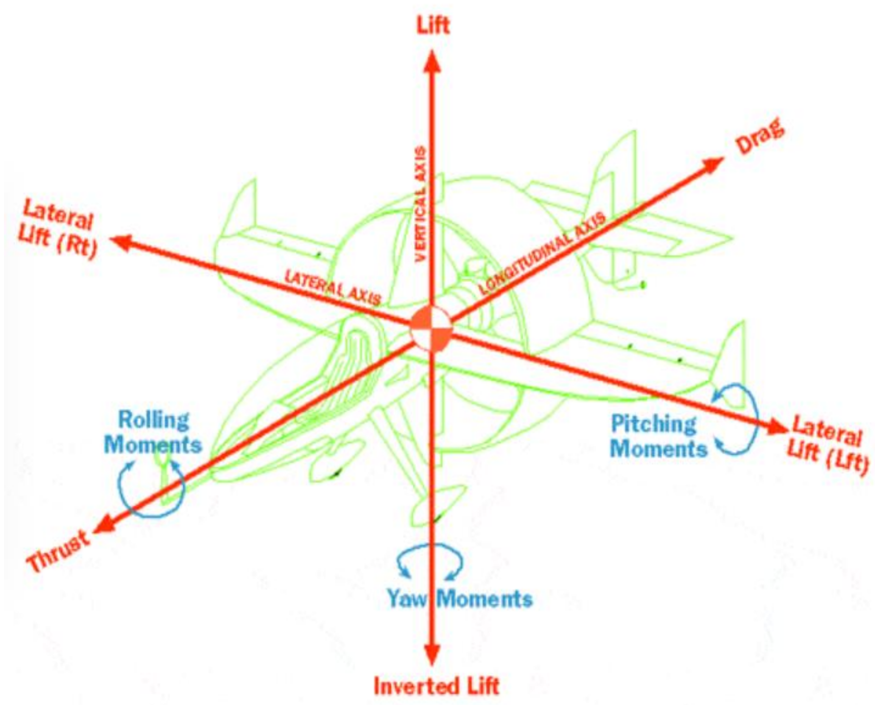

Figure 2.1 Forces and Moments on aircraft (Shaji, 2015).

2.2.2 Axes of an Aircraft

An axis is an imaginary line around which a body rotates. During flight, an aircraft's attitude changes in three dimensions. Flight control is used by the pilot to cause the aircraft to rotate around one or more of its three axes of rotation. The three axes are longitudinal, lateral, and vertical. All three axes intersect at the center of gravity and are perpendicular to each other. The longitudinal axis of an aircraft is the axis that runs from nose to tail and through the fuselage. The lateral axis of an aircraft is the crosswise axis that extends from wing tip to wing tip. The vertical axis is the axis that runs from top to bottom through the center of an aircraft (Shaji, 2015).

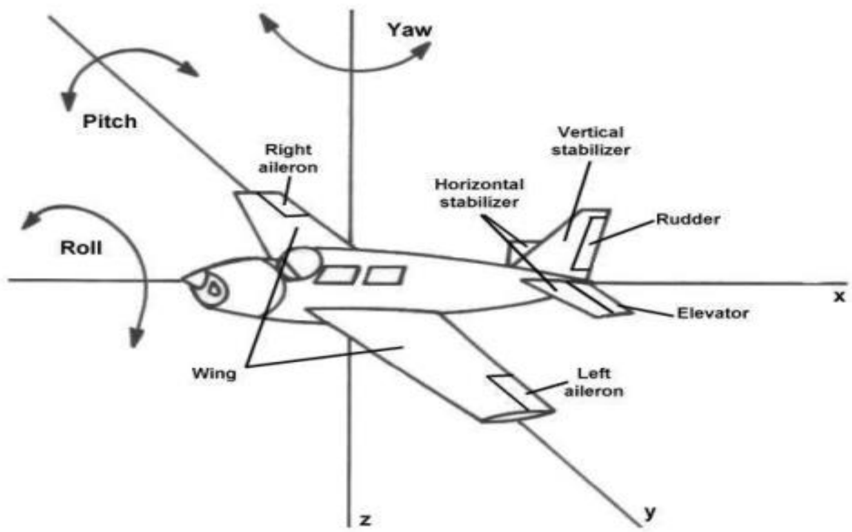

Figure 2.2 Motion of an Aircraft about its axes (Khalid et al., n.d.).

Roll is the motion of an aircraft about its longitudinal axis. Pitch is the motion of an aircraft along its lateral axis. Finally, yaw refers to an aircraft's rotation about its vertical axis. The yaw angle is the angle formed by the north and the projection of the aircraft longitudinal axis onto the horizontal plane. Roll angle is the rotation around the aircraft longitudinal axis after yaw and pitch rotation. Pitch angle is the angle formed by the longitudinal axis and the horizon. An aircraft's roll, pitch, and yaw motion are controlled by three control surfaces: ailerons, elevator, and rudder. Their motion is controlled by ailerons for roll, elevators for pitch, and rudders for yaw (Thanu, 2016).

The angle of attack is the angle formed by the oncoming air or relative wind and the aircraft's reference line. The flight path angle is the angle formed by the aircraft's flight path vector and the local atmosphere (John, 2016).

2.2.3 Flight Control System

The pilot can use the flight control system to control the forces acting on an aircraft, as well as the aircraft's direction and attitude. The fundamental flight control system is made up of a number of mechanical components that have been present in early aircraft.

There are primary and secondary systems in the aircraft control system. Ailerons, elevator, and rudder make up the primary control system, which controls an aircraft safely while in flight. The secondary control systems include the trim system, spoilers, leading edge devices, and wing flaps (Duncan, 2016).

The aerodynamic forces of an aircraft must be controlled by the primary control system in order to follow the reference path. The motion of primary flight control surfaces affects the airflow and pressure distribution over and around the airfoil. These effects can have an impact on the airfoil's lift and drag. This allows the pilot to control an aircraft's three axes of rotation (Hamid & Babar, 2019).

The flight control surface elevator controls the up and down movement of an aircraft's nose. It is associated with the horizontal stabilizer. Elevator controls the pitch of an aircraft about its lateral axis. The pilot deflects the elevator by pulling back on the control stick. This causes the aircraft and the airflow to rise, forcing the tail down and the nose up, increasing the pitch angle. The pilot deflects the elevator down by pushing the control stick forward. This increased the airflow to the tail, decreasing the pitch angle and causing the aircraft's nose motion to dive (Duncan, 2016).

The ailerons on the flight control surface are used to control roll about the longitudinal axis. They move in opposing directions while being affixed to the trailing edge of each wing. Aileron on the opposite side must be up if one is down. Right ailerons deflect upward when pressure is applied to the right, while left ailerons deflect downward. After that, the aircraft rolls to the right. The downward movement of the left aileron increases the angle of attack and wing camber. The upward movement of the right aileron reduces the angle of attack and wing camber. The aircraft rolls to the right due to the difference in forces between increased lift on the left wing and decreased lift on the right wing (Duncan, 2016).

A rudder is a flight control surface used to control an aircraft's motion about its vertical axis. This motion is known as yaw. A movable surface rudder is connected to a fixed surface vertical stabilizer. Rudder movement is controlled by the left and right rudder pedals. Control cables connect the rudder and rudder pedals. To yaw the aircraft right or left, the pilot steps on the rudder pedals and moves the rudder on the tail in the direction of the turn. To produce a coordinated turn, the pilot moves the control stick to the side to up or down the ailerons on the wings (Duncan, 2016).

2.3 Related Works on an Aircraft Pitch Control

The literatures reviewed on this specific thematic area are presented below focused on the different types of controller techniques with different the system performance was investigated.

The authors of (Shaji, 2015) describes how the Dynamic Inversion idea and PID controllers can be used to adjust airplane pitch while the aircraft is travelling. When creating flight controllers, the set of existing or unwanted dynamics is cancelled out and replaced by a set of desired dynamics selected by the designer. This process is known as dynamic inversion. The findings for an aviation aircraft employing standard step response criteria are provided after the suggested PID and PID with dynamic inversion controllers are put into practice. Simulation results demonstrate that PID with Dynamic Inversion controller offers superior performance and higher stability than PID controller for controlling the pitch angle of an aircraft system. The investigation reveals that the PID with Dynamic Inversion has significant percentage overrun and settling time. As a result, the creation of more sophisticated and reliable control methods that can manage aircraft pitch is necessary.

The Author in (Sudha & Deepa, 2016) proposed traditional tuning techniques that centered on optimizing PID control parameters for aircraft dynamics pitch control. In this study, a PID controller is employed to enhance the system performance and stability analysis of an aircraft pitch control. Different traditional tuning techniques, including the Zeigler-Nichols method (ZN), modified Zeigler-Nichols method, Tyreus-Luyben tuning, and Astrom-Hagglund tuning, are used to determine the best PID controller values. The simulation outcomes demonstrate that ZN method PID controller parameter tuning for general aviation aircraft pitch control enhances flight stability and performance more than alternative approaches. Nevertheless, based on the simulation results in this work, it was not possible to accomplish the resilience of the PID controller against disturbances and parameter fluctuations. Additionally, the results of utilizing the improved PID controller with standard tuning techniques show a considerable overshoot.

For aircraft pitch control (Arrosida & Echsony, 2017) also proposed an aircraft pitch control design using observer-state feedback control. The proposed controller has been tested and results confirm the effectiveness of elevator control which makes the nose of the aircraft ascending or descending. The proposed controller which, by means of the control action, is able to regulate a control system controlling the slope of the x-axis or pitch with the observer-state feedback to keep the aircraft always in the position set point, the stabilization of the pitch angle. The main drawback of the paper is it uses linearized aircraft dynamics and linear controller and it doesn't consider robustness to parameter variation and disturbance.

For airplane pitch control, the study in (Patel, 2007) proposed a robust quantitative feedback theory controller design. The suggested control systems have been put into practice in a simulated environment using Matlab and Simulink. Performance of the control system has been evaluated in terms of time domain specification. The outcomes demonstrate the capability of QFT controllers and GA-based QFT controllers to effectively manage the impact of system disruptions. The system replies demonstrate that a pitch control system using a QFT controller performs better than a self-tuning fuzzy PID controller. However, by including a further element to the management system and then putting the control plan into action, more effort can be invested.

For airplane pitch control, conventional PID, adaptive PID, and sliding Mode controllers were suggested in (Khalid et al., n.d., 2019). The suggested system is used to compare traditional PID, fuzzy PID, and sliding mode approaches, and simulation results are reported. The methods stated demonstrate that the performance of SMC and Fuzzy PID is clearly better than that of conventional PID. The proposed Fuzzy PID controller's main feature is that it turns the control parameters during run time because the controller's parameters are constantly updated based on the input error signal. SMC response, on the other hand, can be tweaked to meet specific needs by altering the controller's parameters. In comparison to classical controllers, the proposed techniques have a better response because they have a shorter rise and settling time. But the paper used linear model and it doesn't work on robustness.

There has been research on neural network-based airplane pitch angle control (Păucă & Mirea, 2017). Several control techniques based on artificial neural networks have been developed to regulate the pitch angle of an airplane. For the process (plant) that will be employed as a controller, the first way uses a determined neural inverse model. While the next two techniques aim to reduce the error between the reference and actual pitch angle value by employing a neural network as a controller and a neural network to give the PID controller parameter based on an online training of a neural network. But it doesn't consider robustness to parameter variation and disturbance.

The authors of (N. Wahid and N. Hassan, 2012) proposed Self-Tuning Fuzzy PID Controller Design for Aircraft Pitch Control. In this study, a self-tuning fuzzy PID controller is created to enhance aircraft system pitch control performance. Starting with a derivation of an appropriate mathematical model to explain the longitudinal motion of an aircraft, the controller is designed based on the dynamic modeling of the system. By choosing the proper fuzzy rules through simulation in Matlab and Simulink, fuzzy logic is utilized to modify each parameter of a proportional-integral-derivative (PID) controller. For a longitudinal dynamic in pitch aircraft's autopilot, a comparison between a traditional PID controller and a self-tuning fuzzy PID controller is researched and assessed. According to simulation data, utilizing self-tuning fuzzy PID instead of a traditional PID controller greatly enhanced the performance of a pitch control system. The paper's primary weakness is that it employs linearized aircraft dynamics and a linear controller while neglecting to take robustness to parameter change and disturbance into account.

The author (Rahul B & Dharani J, 2019) proposed genetic algorithm tuned PID controller for aircraft pitch control. By altering the gain in the loop, changes in the aircraft's attitude will have an impact on the transient response. To improve the vehicle's performance, the controller needs to be able to adapt to changes both internally and externally. This work uses a genetic algorithm to create a self-adaptive controller that modifies the control settings based on measurements and analyses of environmental conditions. By fine-tuning the PID controller using a genetic algorithm, this self-adaptive controller for the pitch control system was created. Time response analysis has been used to compare the performance of the conventional PID controller, fuzzy logic-based PID controller, and genetic algorithm-based PID controller. The findings demonstrate that the suggested controller is more effective than conventional controllers and best suited for the efficient operation of the vehicle. However, extra work can be put forward by adding a second component to the management system before implementing the control plan.

There has been research on Flight-Path Tracking Control of an Aircraft Using Backstepping Controller (Kada, Z. O., & Mohamed, T., 2015). In this study, a nonlinear aircraft model's law was designed using a nonlinear backstepping technique. When a controller is applied, the error exponentially converges, allowing the system to become globally stabilised or reach a new equilibrium state. The controller was designed to track angle of attack, pitch angle, and flight route using angular rate. The issue of path angle control for a transportation aircraft has been dealt with. After carefully choosing the states to include and using the appropriate approximations, a nonlinear model representing the longitudinal motion in a strict feedback structure was developed. A nonlinear controller with five free parameters was created by iteratively designing a backstepping control law in three steps. The Lyapunov theory is used to evaluate the closed loop stability of the error states and the parameters of the backstepping technique, and it is demonstrated that the error will automatically converge to a compact set whose size is adjustable by the design parameters. Last but not least, a nonlinear simulation of an aircraft manoeuvre is carried out to show how well the suggested control principles work. But it doesn’t consider robustness to parameter variation and disturbance.

The authors (C. Radhakrishnan & A. Swarup, 2020) proposed the Performance Comparison for Fuzzy based Aircraft Pitch using Various Control Methods. In this paper, two different tuning strategies for a simple PID controller for aeroplane pitch control have been discussed. The other control systems used to achieve pitch control include LQR and Pole placement. The two different PID controller tunings discussed are fuzzy tuning and optimum tuning. These are put into practise using MATLAB. The PID controllers were tuned for the specified control objectives. For arbitrary chosen Q and R matrices, the feedback gain vector for LQR control was obtained, and the system response was examined. Additionally examined was LQR control with GA optimisation. Similar to this, the desired poles were achieved using the Pole Placement Method, achieving the given control objectives. By simulation, it has been found that all of the discussed controllers contribute to performance that is acceptable. lso, these methods contribute a lot of robust performance, so even if the parameters change, the outcome is not significantly worse. Fuzzy PID performs better and demonstrates strong robustness. This study will be useful in determining the best control and tuning strategy to use in order to get a stable and reliable pitch performance. But it doesn't consider the external disturbance effect on the control system.

From the literature reviewed, it is observed that most of the researchers try to minimize the error and improve transient response by using different techniques. But they didn't work on robust control to parameter variation and external disturbance. In this research work, super-twisting sliding mode controller tuned by PSO using ITAEU is applied to aircraft pitch control system.

CHAPTER THREE

METHODOLOGY AND SYSTEM MODELING

3.1 Chapter Overview

This chapter presents the methodology, material and mathematical model of an aircraft system.

3.2 Materials

In this thesis work, software such as MATLAB 2020a, Microsoft office 2016 and Math Type 6.0 equation editor are used. MATLAB is computing software consists of technical toolboxes and Simulink. Microsoft office is used for editing the thesis documentation. Math Type is used for writing mathematical formulas and equations In Microsoft office word and PowerPoint presentation tools.

3.3 Methods

The following methods are used to analyze the objective of the proposed thesis study. First, the theoretical background, closely related papers, and literatures are reviewed. The relevant data used in this thesis work is then collected and analyzed. Then, the mathematical model of an aircraft system is derived. Following that, the Super-twisting sliding mode controller is designed to control the pitch of an aircraft system. Then after, the system is simulated with MATLAB/ Simulink, and the proposed system result is analyzed and compared to the SMC controller. Finally, the thesis work is concluded and recommendations are made for future work. The methodology for this research work is summarized in the block diagram in Figure 3.1.

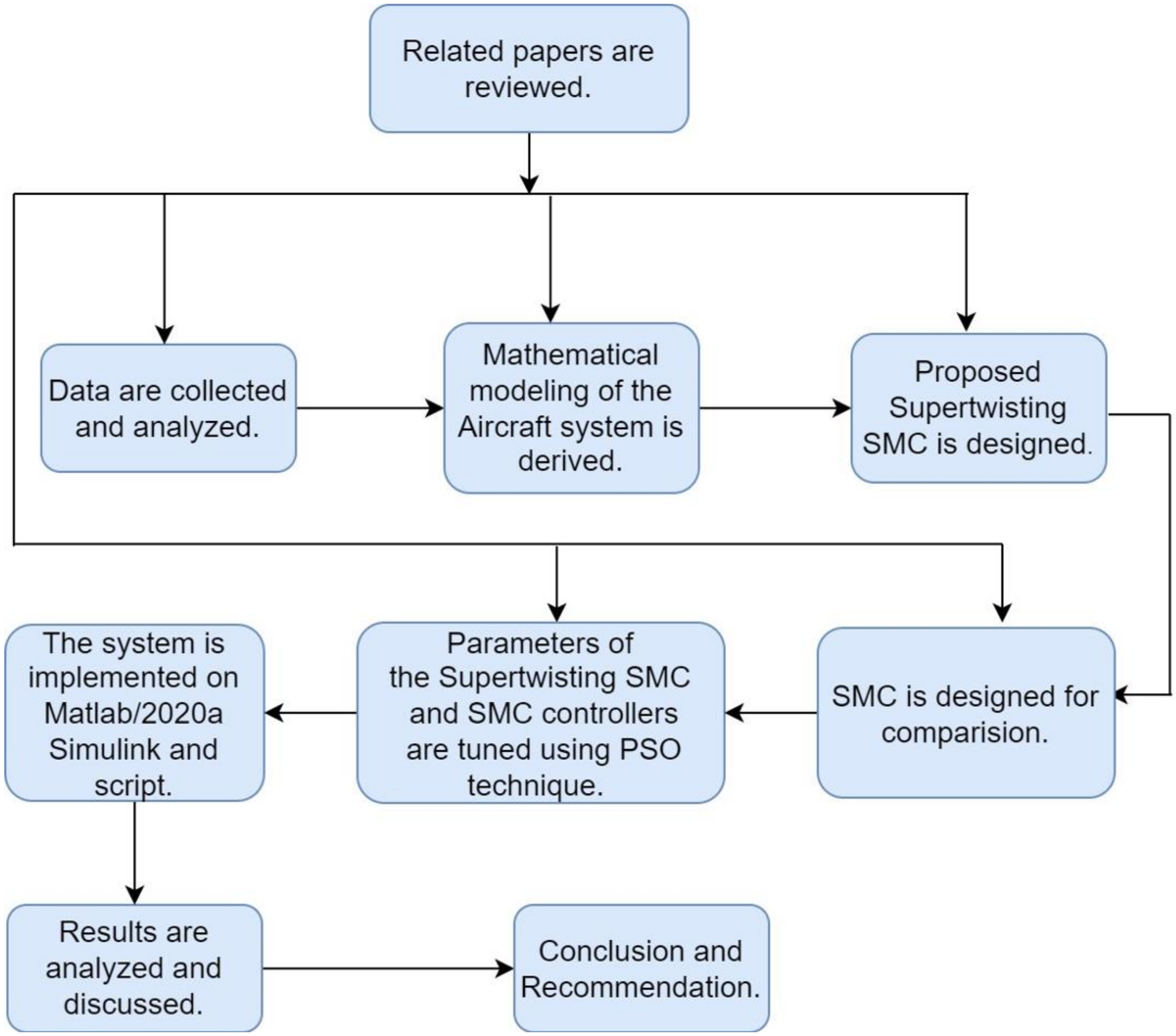

Figure 3.1 Block diagram of the research methodology.

3.4 Mathematical Modeling of an Aircraft System

Using Newton's second law, the equation for an aircraft's motion is created from a rigid aircraft. According to Newton's second law, the sum of the applied forces and moments acting on an object over time equals the rate at which its linear momentum changes over time and the rate at which its angular momentum changes over time.

Definition of aircraft state vector **Forces and moments**

$$\begin{bmatrix} X \\ Y \\ Z \\ L \\ M \\ N \end{bmatrix} = \begin{bmatrix} \textit{Longitudinal}\ \text{Force} \\ \textit{Transverse}\ \text{force} \\ \textit{Vertical}\ \text{force} \\ \textit{Roll}\ \text{moment} \\ \textit{Pitch}\ \text{moment} \\ \textit{Yaw}\ \text{moment} \end{bmatrix}$$

$$v = \begin{bmatrix} u \\ v \\ w \\ p \\ q \\ r \\ \end{bmatrix} = \begin{bmatrix} \textit{Longitudianl}(\textit{forward})\ \text{velocity} \\ \textit{lateral}(\textit{transverse})\ \text{velocity} \\ \textit{Vertical}\ \text{velocity} \\ \textit{Roll Rate} \\ \textit{Pitch}\ \text{Rate} \\ \textit{Yaw}\ \text{Rate} \\ \end{bmatrix}$$

$$\eta = \begin{bmatrix} x_e \\ y_e \\ z_e \\ \phi \\ \Theta \\ \Psi \end{bmatrix} = \begin{bmatrix} \textit{Earth}\ \text{fixed x- position} \\ \textit{Earth}\ \text{fixed y- position} \\ \textit{Earth}\ \text{fixed z- position, Altitude} \\ \textit{Roll}\ \text{angle} \\ \textit{Pitch}\ \text{angle} \\ \textit{Yaw}\ \text{angle} \end{bmatrix}$$

3.4.1 Aircraft Axis System

Three axis system (Ibrahim, 2013):

1. Body axis system: fixed to the aircraft
2. Earth axis system: assume to be inertial axis system fixed to the earth.
3. Stability axis system: defined with respect to the relative wind.

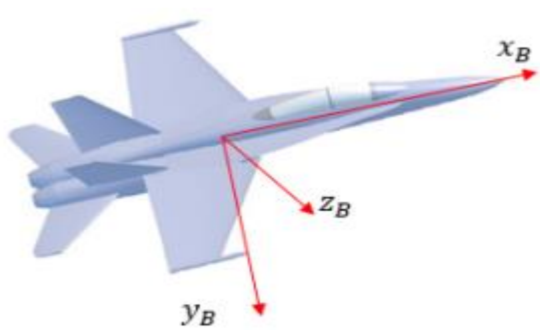

Figure 3.2 Body axis system (Thanu, 2016).

Wind Axis System

The wind axis system (x_w, y_w, z_w) is defined with respect to relative wind. When the side slip angle β is zero, the wind axis become stability axis.

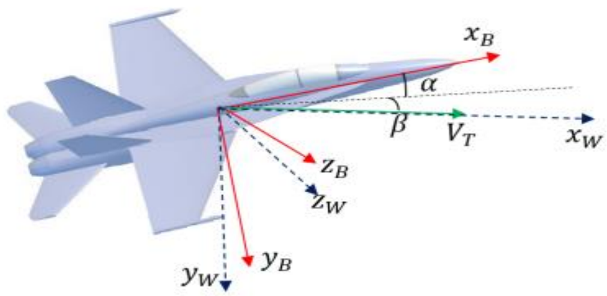

Figure 3.3 Wind axis system (Thanu, 2016).

where α is the angle of attack and β is the side slip angle.

$$\tan(\alpha) = \frac{W}{V}, \quad \sin(\beta) = \frac{V}{V_T} \qquad 3.1$$

where , V_T is the total speed of the aircraft represented by the following equation.

$$V_T = \sqrt{U^2 + V^2 + W^2} \qquad 3.2$$

3.4.2 Axis Transformation

Earth axis to body axis: transforming vector requires three consecutive rotations about the z axis, y axis and x axis respectively.

Stability axis to body axis: useful in transforming the aerodynamic forces from their convenient axis into the body axis system. This is accomplished by rotating the stability axis system through a positive angle of attack (Ibrahim, 2013).

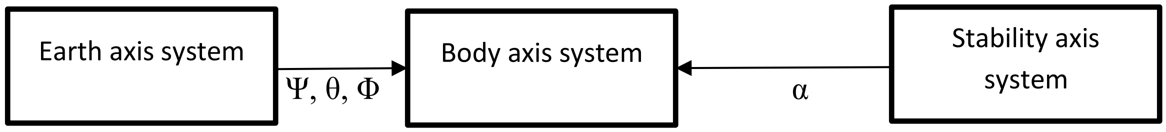

Figure 3.4 Axis transformations (Ibrahim, 2013).

3.4.4 Rotation matrices for wind and stability axis

First, the body fixed coordinate system is rotated at negative side slip angle $-\beta$ about z-axis. Secondly, the new coordinate system is rotated a positive angle of attack α about y-axis such that the resulting x- axis points in the direction of the total speed V_T. Therefore the first rotation defines the wind axis and the second rotation defines the stability axis (Repository, 2013).

$$P^{wind} = R_{z,-\beta} P^{stab} = \begin{bmatrix} C\beta & S\beta & 0 \\ -S\beta & C\beta & 0 \\ 0 & 0 & 1 \end{bmatrix} P^{stab} \qquad 3.3$$

$$P^{stab} = R_{y,\alpha} P^{body} = \begin{bmatrix} C\alpha & 0 & S\alpha \\ 0 & 1 & 0 \\ -S\alpha & 0 & C\alpha \end{bmatrix} P^{body} \qquad 3.4$$

For simplicity *cosine* and *sine* functions are denoted by C and S respectively.
The rotation matrix become:

$$R_{body}^{wind} = R_{z,-\beta} R_{y,\alpha} = \begin{bmatrix} C\alpha C\beta & S\beta & S\alpha C\beta \\ -C\alpha S\beta & C\beta & -S\alpha S\beta \\ -S\alpha & 0 & C\alpha \end{bmatrix} \qquad 3.5$$

$$P^{wind} = R_{body}^{wind} P^{body} \qquad 3.6$$

$$P^{body} = (R_{body}^{wind})^T P^{wind} \qquad 3.7$$

3.4.5 Transformation Matrices for Translation Velocities

The transformation matrices for translation velocities is given by (Bouadi et al., 2014):

$$R_{abc}^{ned} = R_\phi R_\Theta R_\Psi = \begin{bmatrix} 1 & 0 & 0 \\ 0 & C\phi & S\phi \\ 0 & -S\phi & C\phi \end{bmatrix} \begin{bmatrix} C\Theta & 0 & -S\Theta \\ 0 & 1 & 0 \\ S\Theta & 0 & C\Theta \end{bmatrix} \begin{bmatrix} C\Psi & S\Psi & 0 \\ -S\Psi & C\Psi & 0 \\ 0 & 0 & 1 \end{bmatrix} \qquad 3.8$$

By simplifying the above equation the final form of transformation matrix R_{abc}^{ned} is become:

$$R_{abc}^{ned} = \begin{bmatrix} C\phi C\Psi & C\Theta S\Psi & -S\Theta \\ C\Psi S\Theta S\phi - C\phi S\Psi & C\phi C\Psi + S\Theta S\phi S\Psi & C\Theta S\phi \\ S\phi S\Psi + C\phi C\Psi S\Theta & C\phi S\Theta S\Psi - C\Psi S\phi & C\Theta C\phi \end{bmatrix} \qquad 3.9$$

$$\begin{bmatrix} \dot{x}_e \\ \dot{y}_e \\ \dot{z}_e \end{bmatrix} = (R_{abc}^{ned})^T \begin{bmatrix} u \\ v \\ w \end{bmatrix} \qquad 3.10$$

$$\begin{bmatrix} \dot{x}_e \\ \dot{y}_e \\ \dot{z}_e \end{bmatrix} = \begin{bmatrix} C\Psi C\Theta & -S\Psi C\phi + C\Psi S\Theta S\phi & S\Psi S\Theta + C\Psi C\phi S\Theta \\ S\Psi C\Theta & C\Psi C\phi + S\phi S\Theta S\Psi & -C\Psi S\phi + S\Theta S\Psi C\phi \\ -S\Theta & C\Theta S\phi & C\Theta C\phi \end{bmatrix} \begin{bmatrix} u \\ v \\ w \end{bmatrix} \qquad 3.11$$

3.4.6 Transformation Matrices for Angular Velocities

The transformation matrices for angular velocities given by (Bouadi et al., 2014):

$$\begin{bmatrix} P \\ Q \\ R \end{bmatrix} = R_\phi R_\Theta \begin{bmatrix} 0 \\ 0 \\ \dot{\Psi} \end{bmatrix} + R_\phi \begin{bmatrix} 0 \\ \dot{\Theta} \\ 0 \end{bmatrix} + \begin{bmatrix} \dot{\phi} \\ 0 \\ 0 \end{bmatrix} \qquad 3.12$$

$$\begin{bmatrix} P \\ Q \\ R \end{bmatrix} = \begin{bmatrix} 1 & 0 & 0 \\ 0 & C\phi & S\phi \\ 0 & -S\phi & C\phi \end{bmatrix} \begin{bmatrix} C\Theta & 0 & -S\Theta \\ 0 & 1 & 0 \\ S\Theta & 0 & C\Theta \end{bmatrix} \begin{bmatrix} 0 \\ 0 \\ \dot{\Psi} \end{bmatrix} + \begin{bmatrix} 1 & 0 & 0 \\ 0 & C\phi & S\phi \\ 0 & -S\phi & C\phi \end{bmatrix} \begin{bmatrix} 0 \\ \dot{\Theta} \\ 0 \end{bmatrix} + \begin{bmatrix} \dot{\phi} \\ 0 \\ 0 \end{bmatrix} \quad 3.13$$

$$\begin{bmatrix} \dot{\phi} \\ \dot{\Theta} \\ \dot{\Psi} \end{bmatrix} = \begin{bmatrix} 1 & S\phi T\Theta & C\phi T\Theta \\ 0 & C\phi & -S\phi \\ 0 & S\phi / C\Theta & C\phi / C\Theta \end{bmatrix} \begin{bmatrix} P \\ Q \\ R \end{bmatrix}, \;\; \mathrm{C}\Theta \neq 0 \quad 3.14$$

3.4.7 Rigid body kinetics

The aircraft rigid body kinetics can be expressed as (Ibrahim, 2013):

$$m(\dot{v}_1 + v_2 \;x\; v_1) = \tau_1 \quad 3.15$$

$$I_{GG}\dot{v}_2 + v_2 \text{ x } (\mathrm{I}_{GG} v_2) = \tau_2 \quad 3.16$$

where $v_1 = [u, v, w]^T$, $\mathrm{v}_2 = [p, q, r]^T$, $\tau_1 = [X, Y, Z]^T$, and $\tau_2 = [L, M, N]^T$.

Assume the aircraft center of gravity (CG) is align with the coordinate system. The model is become:

$$M_{RB}\dot{v} + C_{RB}(v)v = \tau_{RB} \quad 3.17$$

where, $M_{RB} = \begin{bmatrix} mI_{3x3} & 0_{3X3} \\ 0_{3x3} & I_{CG} \end{bmatrix}$, $\mathrm{C}_{RB}(v) = \begin{bmatrix} mS(v_2) & 0_{3x3} \\ 0_{3X3} & -S(I_{CG} v_2) \end{bmatrix}$.

The moments and forces applied on aircraft can be expressed as:

$$\tau_{RB} = -g(\eta) + \tau \quad 3.18$$

Where τ is a vector of aerodynamics and control forces.

The gravitational forces acts in the center of gravity expressed in NED as follows:

$$f_G = \begin{bmatrix} 0 \\ 0 \\ mg \end{bmatrix} \quad 3.19$$

The gravitational force provides the following vector:

$$g(\eta) = -(R_{abc}^{ned})^T \begin{bmatrix} f_G \\ 0_{3x1} \end{bmatrix} = \begin{bmatrix} mg\sin(\Theta) \\ -mg\cos(\Theta)\sin(\Phi) \\ -mg\cos(\Theta)\cos(\phi) \\ 0 \\ 0 \\ 0 \end{bmatrix} \quad 3.20$$

Therefore, the aircraft model can be expressed as (Repository, 2013):

$$M_{RB}\dot{v} + C_{RB}(v)v + g(\eta) = \tau \quad 3.21$$

In component form the aircraft model become:

$$X = m\left(\dot{u} + qw - rv + g\sin(\Theta)\right) \quad 3.22$$

$$Y = m\left(\dot{v} + ur - wp - g\cos(\Theta)\sin(\phi)\right) \quad 3.23$$

$$Z = m\left(\dot{w} + vp - qu - g\cos(\Theta)\cos(\phi)\right) \quad 3.24$$

$$L = I_x\dot{p} - I_{xz}(\dot{r} + pq) + (I_z - I_y)qr \quad 3.25$$

$$M = I_y\dot{q} + I_{xz}(p^2 - r^2) + (I_x - I_z)pr \quad 3.26$$

$$N = I_z\dot{r} - I_{xz}\dot{p} + (I_y - I_x)pq + I_{xz}\mathrm{qr} \quad 3.27$$

For the control of pitch of an aircraft, the six aircraft equations can be decoupled into sets of three equations. There are three longitudinal equation of motions and three lateral directional equation of motions.

Assume an aircraft is in wings level flight with no sideslip or no lateral direction motion, the pitching motion can be analyzed using only the longitudinal equation of motions. With this assumption the nonlinear longitudinal dynamics of the aircraft can be written in the body frame as:

$$X = m\left(\dot{u} + qw + g\sin(\Theta)\right) \quad 3.28$$

$$Z = m\left(\dot{w} - qu - g\cos(\Theta)\right) \quad 3.29$$

$$M = I_y\dot{q} \quad 3.30$$

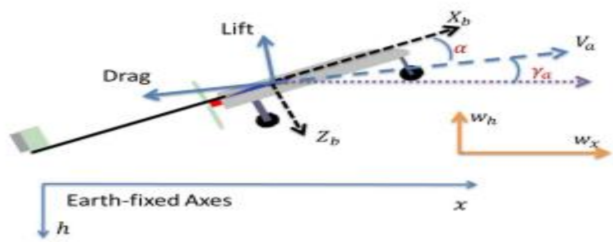

Figure 3.5 System coordinates, angles and aerodynamic forces (Cunjia & Wen, 2016).

The longitudinal equation motion of an aircraft in wind reference frame can be expressed in terms of angle of attack α, sideslip angle β and airspeed $v_a$variable given by (Bouadi et al., 2014):

$$u = v_a \cos\alpha \cos\beta \tag{3.31}$$

$$v = v_a \sin\beta \tag{3.32}$$

$$w = v_a \sin\alpha \cos\beta \tag{3.33}$$

$$\alpha = \theta - \gamma \tag{3.34}$$

Therefore, the longitudinal equation of motions of an aircraft in the wind reference frame become:

$$\dot{x} = v_a \cos\gamma \tag{3.35}$$

$$\dot{z} = -v_a \sin\gamma \tag{3.36}$$

$$\dot{v}_T = \frac{1}{m}(-D + T\cos\alpha - mg\sin\gamma) \tag{3.37}$$

$$\dot{\alpha} = q + \frac{1}{mv_a}(-L - T\sin\alpha + mg\cos\gamma) \tag{3.38}$$

$$\dot{\gamma} = \frac{1}{mv_a}(T\sin\alpha + L - mg\cos\gamma) \tag{3.39}$$

$$\dot{\Theta} = q \tag{3.40}$$

$$\dot{q} = \frac{1}{I_{yy}} M \tag{3.41}$$

3.4.8 State Space Equation for an Aircraft Longitudinal Dynamics

There are 7 state equation that represent the longitudinal dynamics of an aircraft and the state vector defined as:

$$x = \left[x_1 \quad \mathrm{x}_2 \quad \mathrm{x}_3 \quad \mathrm{x}_4 \quad \mathrm{x}_5 \quad \mathrm{x}_6 \quad \mathrm{x}_7 \right]^T$$

The state variables are $x = \left[x \quad z \quad v_a \quad \alpha \quad \gamma \quad \Theta \quad q \right]$ and the state space equation become:

$$\dot{x}_1 = x_3 \cos x_5 \qquad 3.42$$

$$\dot{x}_2 = -x_3 \sin x_5 \qquad 3.43$$

$$\dot{x}_3 = \frac{1}{m}(-D + T \cos x_4 - mg \sin x_5) \qquad 3.44$$

$$\dot{x}_4 = x_7 + \frac{1}{mx_3}(-L - T \sin x_4 + mg \cos x_5) \qquad 3.45$$

$$\dot{x}_5 = \frac{1}{mx_3}(T \sin x_4 + L - mg \cos x_5) \qquad 3.46$$

$$\dot{x}_6 = x_7 \qquad 3.47$$

$$\dot{x}_7 = \frac{M}{I_{yy}} \qquad 3.48$$

Where, $D = \frac{1}{2}\rho {v_a}^2 s_c c_d$,

$$L = \frac{1}{2}\rho {v_a}^2 s_c (c_{l0} + c_{l\delta h}\delta_h + \frac{\tilde{c}}{2v_a} c_{lq} q)$$, and

$$M = \frac{1}{2}\rho {v_a}^2 s_c (c_{m0} + c_{m\delta h}\delta_h + \frac{\tilde{c}}{2v_a} c_{mq} q)$$.

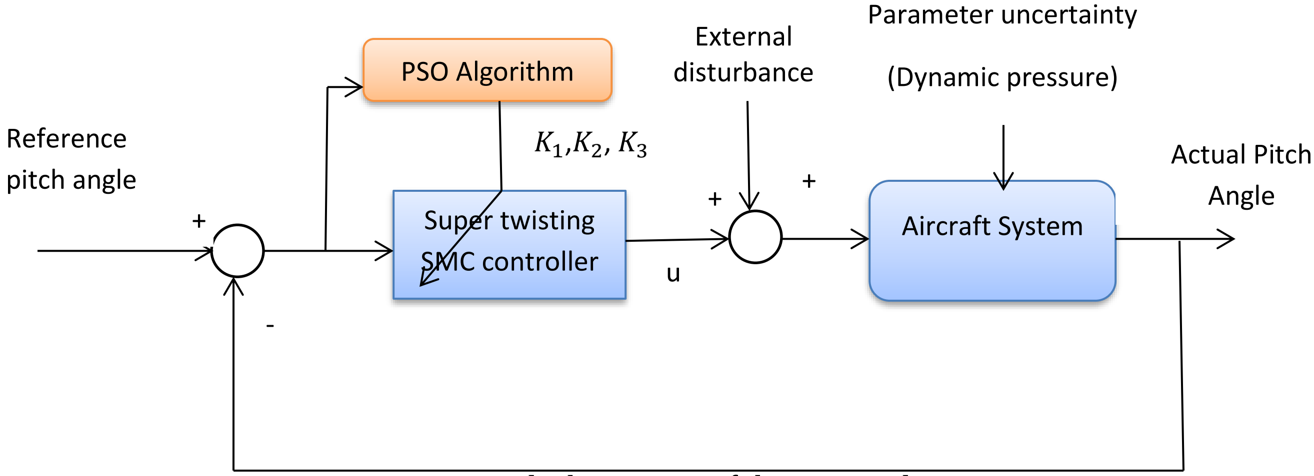

Figure 3.6 Block Diagram of the proposed system.

3.5 Open Loop Analysis of the system

The open-loop control of the aircraft pitch mechanism acts solely on the basis of an input, and the control action is unaffected by the output. Figure 3.7 shows the open loop response of the aircraft's pitch to a step signal in the absence of a controller. Figure 3.7's open loop response shows the system's diverging free response.

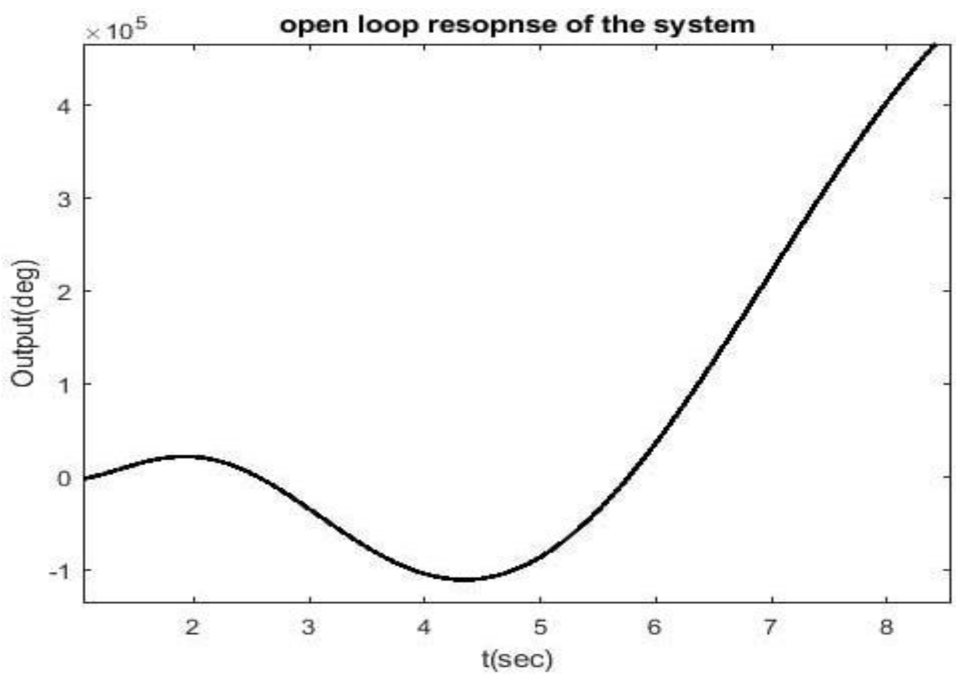

Figure 3.7 open loop response of the system.

CHAPTER FOUR

CONTROLLER DESIGN

4.1 Chapter Overview

This chapter provides a brief explanation of the proposed super-twisting sliding mode controller and the traditional sliding mode controller. Also presented is the particle swarm optimization (PSO) algorithm, which bases its operation on reducing the suggested objective function.

4.2 Sliding Mode Controller

The most well-known and prejudice kit for robust control of nonlinear system is called sliding mode control. Robustness to uncertainty is the most important point in control system design. SMC is robust to control linear and nonlinear system based on the principle of variable structure control. The control signal is discontinuous, switching one or more manifolds in state space is the main property of variable structure control (VSS). When the state cross each discontinuity surface the structure of the feedback system is changed. Figure 4.1 shows that the graphical interpretation of SMC using phase plane, which is made up of error and its derivative. It starts from any initial point, the state trajectory reaches the surface within finite time called reaching mode, and the slides along the surface towards the target called sliding mode (Sivaramakrishna & Santhi, 2017).

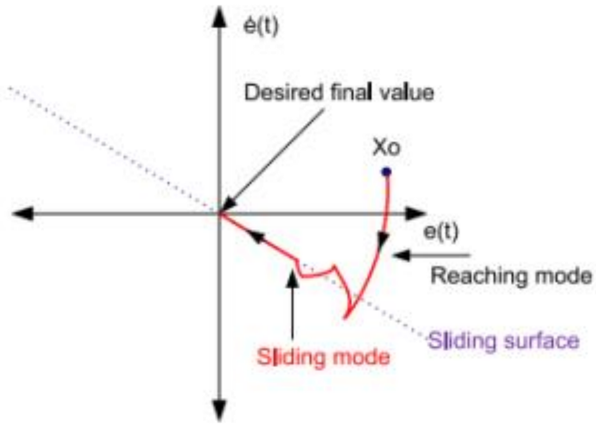

Figure 4.1 Graphical interpretation of SMC (Sivaramakrishna & Santhi, 2017).

The first step of SMC design is design of custom made surface. The plant dynamics is restricted to the equation of surface and is robust to plant match plant uncertainties and external disturbances on the sliding surface (Sivaramakrishna & Santhi, 2017).

The second step is design a hitting control law such that to provide the system trajectory forced to reach to the sliding surface and remains on this surface in the subsequent time once intercepted (Sivaramakrishna & Santhi, 2017).

The pure SMC has the following drawback in practical application. Firstly, it introduces high frequency of oscillation called chattering. Secondly, SMC is susceptibility to measurement noise. The input is based on the sign of measured variable which is close to zero, the point where measurement noise enters the scheme with unfavorable effect. Thirdly, to handle parametric uncertainties the SMC can employ large control signal (Erbatur et al., 2001).

To overcome the above mentioned problems many arrangements are introduced on the pure SMC, one of the best combination is dealing with higher order SMC. In this thesis second order SMC called Super-Twisting SMC is introduced.

4.3 Super-Twisting Sliding Mode Control

Using sign function in equation (4.8) can induce high frequency trajectory chattering around the sliding surface and leading to the system output oscillation around the reference values and the other characteristics of SMC is that the convergence of system states to the equilibrium is not in a finite time but it is asymptotical (Y. Li & Peng, 2021).

Therefore to overcome the above mentioned problem the super-twisting sliding mode control system is introduced.

The STSMC is provide robustness and can eliminate chattering, while providing high precision. In the design process of STSMC the output of the sliding variable is required so, it makes simple in terms of computation burden (Lee et al., 2018).

In this thesis, a super-twisting sliding mode (STSMC) controller is used to control the pitch of an aircraft with SMC robustness. In this method, a super-twisting method substitutes the sign function to smooth the control operation.

4.4 Sliding Mode Control for an aircraft pitch control

To design a control signal $y(t) = x_6(t) = \Theta$ as output measurement and $y_r(t) = \Theta_r$ as a desired signal.

The tracking error and its rate of change are defined as (Sivaramakrishna & Santhi, 2017):

$$e = y_r - y = \Theta_r \text{-} \Theta \qquad 4.1$$

$$\dot{e} = \dot{y}_r - \dot{y} = \dot{\Theta}_r - \dot{\Theta} \qquad 4.2$$

The objective is to enforce $e(t) \to 0$ such that $y \to y_r$ as $t \to \infty$.

The sliding surface called switching function is defined as (Erbatur et al., 2001):

$$s = \dot{e} + k_1 e \qquad 4.3$$

The SMC structure is consists of switching and equivalent control as defined in Equation (4.4) below (Sivaramakrishna & Santhi, 2017):

$$u = u_{eq} + u_{sw} \tag{4.4}$$

Where u_{sw} is the switching control that involved when $s(e,t) \neq 0$, corresponds to the reaching phase. And u_{eq} is the equivalent control corresponds to sliding phase when $s(e,t) = 0$.

The equivalent control, u_{eq} is derived by solving the first derivative of sliding surface i.e. $\dot{s}(e,t) = 0$ at every $t > t_0$ for some t_0, so it is obtained as:

$$\dot{s}(e,t) = 0 \tag{4.5}$$

$$\ddot{e} + k_1\dot{e} = 0 \tag{4.6}$$

Substituting equation (4.2) into equation (4.6) gives as:

$$\ddot{\Theta}_r - \ddot{\Theta} + k_1\dot{\Theta}_r - k_1\dot{\Theta} = 0 \tag{4.7}$$

Since $\ddot{\Theta} = \dot{q}$ substitute equation (3.47) into equation (4.7) gives as:

$$\ddot{\Theta}_r - \dot{q} + k_1\dot{\Theta}_r - k_2\dot{\Theta} = 0 \tag{4.8}$$

$$\ddot{\Theta}_r - [\frac{1}{2I_y}\rho v_a{}^2 s_c(c_{m0} + c_{m\delta h}u_{eq} + \frac{\tilde{c}}{2v_T}c_{mq}q)] + k_1\dot{\Theta}_r - k_1\dot{\Theta} = 0 \tag{4.9}$$

The equivalent control signal become:

$$u_{eq} = \frac{2I_y}{\rho v_a{}^2 s_c c_{m\delta h}}[\ddot{\Theta}_r + k_1\dot{\Theta}_r - k_1\dot{\Theta}] - \frac{\tilde{c}}{2v_a c_{m\delta h}}c_{mq}q - \frac{c_{m0}}{c_{m\delta h}} \tag{4.10}$$

And, u_{sw} is designed to minimize the interference caused by time varying parameter or external disturbance to ensure system motion in sliding mode. It is designed as:

$$u_{sw} = \lambda\,\mathrm{sgn}(s) \tag{4.11}$$

where, $\mathrm{sgn}(s)$ is a sign function defined as: $\mathrm{sgn}(s) = 1$ when, $s > 0$ or $\mathrm{sgn}(s) = -1$ when, $s < 0$.

Here, the control signal is the combination of equivalent control and switching control then the final SMC control signal is obtained by substituting equation (4.10) and (4.11) into equation (4.4) and the control signal become:

$$u = u_{eq} + u_{sw} = \frac{2I_y}{\rho v_a{}^2 s_c c_{m\delta h}}[\ddot{\Theta}_r + k_1\dot{\Theta}_r - k_1\dot{\Theta}] - \frac{\tilde{c}}{2v_a c_{m\delta h}} c_{mq} q - \frac{c_{m0}}{c_{m\delta h}} \text{ -}\lambda\,\mathrm{sgn}(s) \qquad 4.12$$

4.5 Stability Analysis

Lyapunov function is selected to analysis the stability of the system and it is defined as (Erbatur et al., 2001):

$$v = \frac{1}{2}s^2 \qquad 4.13$$

It guarantees that the system trajectory directs towards the switching surface on either side of $s(e,t) = 0$. The system defined in equation (4.8) is stable if and only if the derivative of Lyapunov function is negative.

$$\begin{aligned}
&\dot{v} < 0 \\
&s\dot{s} < 0 \\
&s(\ddot{e} + k_1\dot{e}) < 0 \\
&s(\ddot{\Theta}_r - \ddot{\Theta} + k_1\dot{\Theta}_r - k_1\dot{\Theta}) < 0 \\
&s(\ddot{\Theta}_r - [\frac{1}{2I_y}\rho v_a{}^2 s_c(c_{m0} + c_{m\delta h}u + \frac{\tilde{c}}{2v_a}c_{mq}q)] + k_1\dot{\Theta}_r - k_1\dot{\Theta}) < 0
\end{aligned} \qquad 4.14$$

Substitute equation (4.12) into equation (4.14) the equation become:

$$s(\ddot{\Theta}_r - [\frac{1}{2I_y}\rho v_a{}^2 s_c(c_{m0} + c_{m\delta h}[\frac{2I_y}{\rho v_a{}^2 s_c c_{m\delta h}}[\ddot{\Theta}_r + k_1\dot{\Theta}_r - k_2\dot{\Theta}] - \frac{\tilde{c}}{2v_a c_{m\delta h}}c_{mq}q - \frac{c_{m0}}{c_{m\delta h}} \text{ -}\lambda\,\mathrm{sgn}(s)]$$

$$+\frac{\tilde{c}}{2v_T}c_{mq}q)] + k_1\dot{\Theta}_r - k_2\dot{\Theta}) < 0 \qquad 4.15$$

Rearrange equation (4.15) gives the following expression:

$$s(\frac{1}{2I_y}\rho v_T{}^2 s_c c_{m\delta h}\lambda\,\mathrm{sgn}(s)) < 0 \qquad 4.16$$

Therefore, all the coefficient of the parameters of the equation (4.16) are positive, except the term $c_{m\delta h,}$ it is negative term so, the derivative of the Lyapunov function is negative. This indicates that the designed control signal is stable.

4.6 Super-Twisting Sliding Mode Control Design for pitch control of an aircraft

The switching control law is designed based on the super-twisting algorithm is given by (Y. Li & Peng, 2021):

$$u_{sw} = -k_2\sqrt{|s|}\,\mathrm{sgn}(s) + v \tag{4.17}$$

$$\dot{v} = -k_3\,\mathrm{sgn}(s) \tag{4.18}$$

Where $k_2$and k_3 are positive constants.

Then the switching control law become

$$u_{sw} = -k_2\sqrt{|s|}\,\mathrm{sgn}(s) - \int k_3\,\mathrm{sgn}(s)dt \tag{4.19}$$

Therefore the final control law using STSMC algorithm obtained as follows:

$$\begin{aligned} u = u_{eq} + u_{sw} = \frac{2I_y}{\rho v_a{}^2 s_c c_{m\delta h}}[\ddot{\Theta}_r + k_1\dot{\Theta}_r - k_1\dot{\Theta}] - \frac{\tilde{c}}{2v_a c_{m\delta h}}c_{mq}q - \frac{c_{m0}}{c_{m\delta h}} \\ -k_2\sqrt{|s|}\,\mathrm{sgn}(s) - \int k_3\,\mathrm{sgn}(s)dt \end{aligned} \tag{4.20}$$

4.7 Optimal Tuning of the Super-twisting Sliding Mode Controller

In the design of super-twisting controller for an aircraft pitch three design parameters such as k_1, k_2 and k_3 are exist. The performance and the stability of the system are directly affected by the design parameters. The optimal values of the parameters are important to achieve the objective of the system. In this thesis work particle swarm optimization (PSO) is used to get the optimal values of the design parameter.

4.7.1 Performance Indices

A variety of performance indices can be used to gauge the overall performance of the control system. By reducing the integral of the error up until the process has reached the target set point, this demonstrated the effectiveness of the controlled reaction.

To attain acceptable system performance characteristics while limiting the control input, an objective function must be properly chosen. The most important stage in the optimization process is choosing the proper goal function. An objective function is frequently referred to as a performance index in the context of control.

The integral of absolute error (IAE), the integral of time multiplied absolute error (ITAE), and the integral of squared error (ISE) are the three typically utilized performance measurements in tuning controller parameters, which are based on error as (J.Jebakumar et al., 2014):

$$
\begin{aligned}
IAE &= \int_0^{t_f} |e(t)| dt \\
ITAE &= \int_0^{t_f} t\,|e(t)| dt \\
ITAE &= \int_0^{t_f} e^2(t) dt
\end{aligned}
\qquad 4.21
$$

Each of the aforementioned measurements is determined during a period of time ranging from $0<t<t_f$, where t_f is the length of time necessary for the error to dissipate.

There are benefits and drawbacks to these performance standards. For instance, ISE tuning results in a quick reaction with low amplitude oscillation and makes large errors larger and minor errors smaller. IAE tends to respond more slowly than ISE tuning and does not give the faults any more weight. ITAE adds increased time weight to the absolute error at later dates and applies a minor time penalty for the initial significant error (Chen et al., 2017).

This thesis work uses the Integral of Absolute Error and Control Signal (IAEU) as the objective function to provide acceptable dynamic characteristics in the transition process while avoiding an excessive control input when the setpoint changes abruptly. It provides information on both setpoint tracking and control effort. It is defined in the following way:

$$IAEU = \int_0^t |e(t)| + w|\Delta u|\,dt \qquad 4.22$$

where $e(t)$ is the error, that is, the difference between the reference signal and actual output with $e(t) = y_r - y$,w= weighting factor and $\Delta u = u - u_0$ which is the deviation of the control input. u is the final value of the control signal. u_0 denotes the control input at an operating point. By altering the weighting factor, the proposed performance index (IAEU) can suit the designer's diverse needs. A critical step in the controller design process is choosing an appropriate weighting factor value.

4.7.2 Particle Swarm Optimization as an optimization tool

Kennedy and Eberhart invented the particle swarm optimization (PSO), a stochastic technique based on swarms, in 1995. This algorithm uses ideas from the social behavior of animals, like a school of fish or a flock of birds. Each potential solution to a given problem is represented by PSO as a particle flying through the problem space at a set speed, much like a flock of birds looking for food. Then, in order to select its subsequent path across the search space, each particle combines some characteristics of its most recent best position, current location, as well as those of one or more swarm agents, with specific random disturbances (Gad, 2022). When all of the particles have been moved, the subsequent iteration starts. Over time, the entire swarm (such as a flock of birds searching for food) will probably become closer to performing at its best. The position (a set of coordinates describing a point in the search space), velocity, and best prior position of each particle serve as its representations. The position (a set of coordinates describing a point in the search space), the best preceding position, and the velocity of each particle serve as its representations. At each iteration of the procedure, particles in their current location are assessed using a fitness function, and if the value of the fitness function is superior than any previously achieved, it is kept as the best position pbest. The closest particle is given the highest fitness function value and is saved as pbest. The particle's next position and velocity are then determined using the formula below(Nakisa et al., 2014), (X.-L. Li et al., 2019):

$$v_i^{t+1} = \omega v_i^t + c_1 r_1 (p_{best} - x_i^t) + c_2 r_2 (g_{best} - x_i^t) \quad 4.23$$

$$x_i^{t+1} = v_i^{t+1} + x_i^t \qquad i = 1, 2, ..., n \quad 4.24$$

where, t is the iteration time, x_i is the particle position in the search space at i^{th} iteration, v_i is the velocity of particle at i^{th} iteration, p_{best} is the personal best position of the particle, g_{best} is the global best position for the PSO, c_1, c_2 are the acceleration coefficients, ω is the weight inertia, and r_1, r_2 are random numbers between 0 and 1.

PSO algorithm for tuning is shown in Figure 4.2, below.

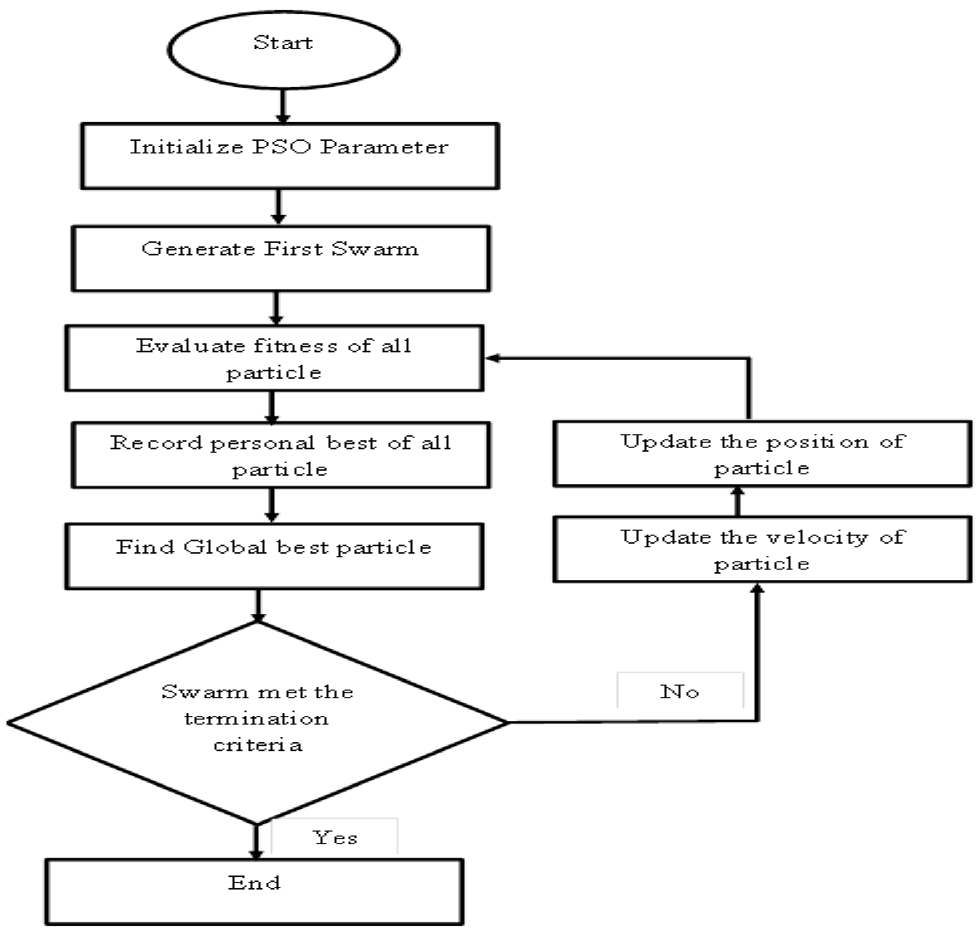

Figure 4.2 Flow Chart of PSO Algorithm

4.8 Controller parameter settings

4.8.1 Parameter Settings for the Sliding Mode Controller

Particle swarm optimization (PSO) algorithm is used to tune the design parameter of sliding mode control k_1 and λ. The details of the PSO parameter setting used in this work is illustrated in the table 4.1 below.

Table 4.1 Parameter settings of the PSO for SMC

Parameter		Value
Swarm size		20
Maximum iteration		30
Number of the parameters		2
Inertia weight	$\omega_{\min}$	0.4
	$\omega_{\max}$	0.9
Acceleration constant	c_1	2
	c_2	2
Lower bounds		[0.0001 0.0001]
Upper bounds		[300 0.1]

The graphical result of the PSO technique for SMC with its best function value is shown in Figure 4.3. The minimum best function value is 4.08613 at iteration 30.

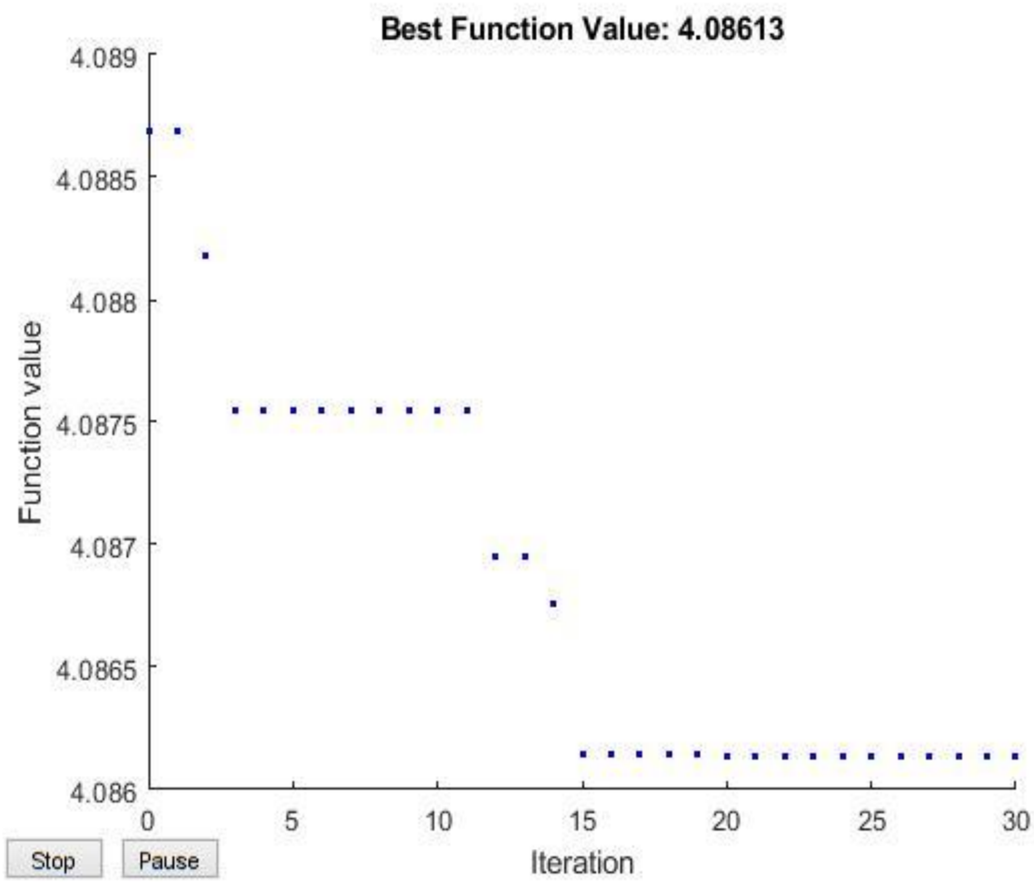

Figure 4.3 Convergence curve of the PSO algorithm for SMC Control

Table 4.2 Optimal values of the SMC gains

Optimization Technique	SMC Gains	
	k_1	λ
PSO	299.0623	0.0808

4.8.2 Parameter Settings for the Proposed Super- Twisting Sliding Mode Controller
Particle swarm optimization (PSO) algorithm is used to tune the design parameter of sliding mode controlk_1, $k_2$andk_3 . The details of the PSO parameter setting used in this work is illustrated in the table 4.3 below.

Table 4.3 Parameter settings of the PSO for STSMC

Parameter		Value
Swarm size		20
Maximum iteration		30
Number of the parameters		3
Inertia weight	$\omega_{\min}$	0.4
	$\omega_{\max}$	0.9
Acceleration constant	c_1	2
	c_2	2
Lower bounds		[0.0001 0.0001 0.0001]
Upper bounds		[300 0.1 0.1]

The graphical result of the PSO technique for SMC with its best function value is shown in Figure 4.4. The minimum best function value is 62.4161 at iteration 30

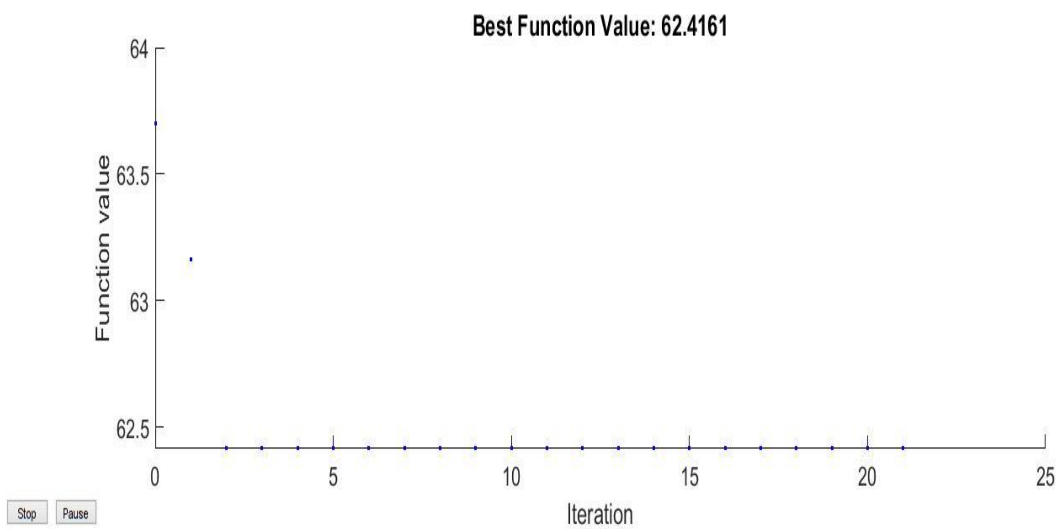

Figure 4.4 Convergence curve of the PSO algorithm for STSMC Control

Table 4.4 Optimal values of the STSMC gains

Optimization Technique	STSMC gains		
	k_1	k_2	k_3
PSO	234.9333	0.0144	0.0535

CHAPTER FIVE

RESULTS AND DISCUSSIONS

5.1 Chapter Overview

This chapter discusses and compares the simulation outcomes of the proposed super-twisting sliding mode controller and sliding mode controller for the aircraft pitch system. The simulation is broken up into two parts in order to demonstrate the usefulness of the suggested control algorithm. The tracking performance of both controllers is assessed in the first portion using the single step, ramp, and up and down signals. The robustness under the influence of dynamic pressure variation and external disturbance force is tested in the second segment. The tracking performance is compared using the proposed performance index (IAEU) and the system's transient response characteristics, such as rise time, peak time, and settling time. Software called MATLAB is used to run the total simulation.

5.2 Parameter Settings of an Aircraft System

The parameters and their values of an aircraft system model used for the simulation works are based on boeing 747- 200 Aircraft which is collected from other related references.

Table 5.1 Geometric parameter of boeing 747- 200 Aircraft (Ahmad et al., 2021).

No	Geometric parameter	Symbol	Value
1	Reference Area	S	$5500 ft^2$
2	Chord	$\bar{C}$	27.3 ft
3	True Air Speed	V	871 ft/sec
4	Dynamic Pressure	ρ	222.8 psi
5	Moment of Inertia	I_{yy}	$3.31*10^7$ slug-ft^2
6	Thrust	T	54750 lbf
7	Mass	m	636636 lbs

Table 5.2 Aerodynamic coefficient of Boeing 747- 200 Aircraft (Ahmad et al., 2021).

No	Parameter	Value
1	c_d	0.0393
2	c_{lo}	0.12
3	$c_{l\delta h}$	0.356
4	c_{lq}	5.13
5	c_{mo}	0.121
6	$c_{m\delta h}$	-1.43
7	c_{mq}	-20.7

5.3 Tracking Performance Tests

This section contrasts the STSMC controller's tracking performance with that of the SMC controller. As tracking references single step, ramp, and multiple step signals are employed. The effectiveness of the controller is assessed by comparing the system's actual output to the reference signals on a graph. Additionally, the tracking effectiveness of the controllers is assessed when load variation and external disturbance force are present.

5.3.1 Tracking performance under normal condition

The tracking capabilities of the proposed STSMC and SMC controllers are discussed in this part for single-step, multiple-step, and ramp signals under typical conditions, that is, without taking the impact of external disturbance and load variation into account.

5.3.1.1 Single step signal

This thesis examines the system response, in particular the pitch angle. Using the STSMC and SMC controller's comparative stability analysis in time domains, the effectiveness of the suggested solution for the system was evaluated. The reaction of a pitch control system for an airplane built using different methods and a desired angle of input of θ_r=10^0.

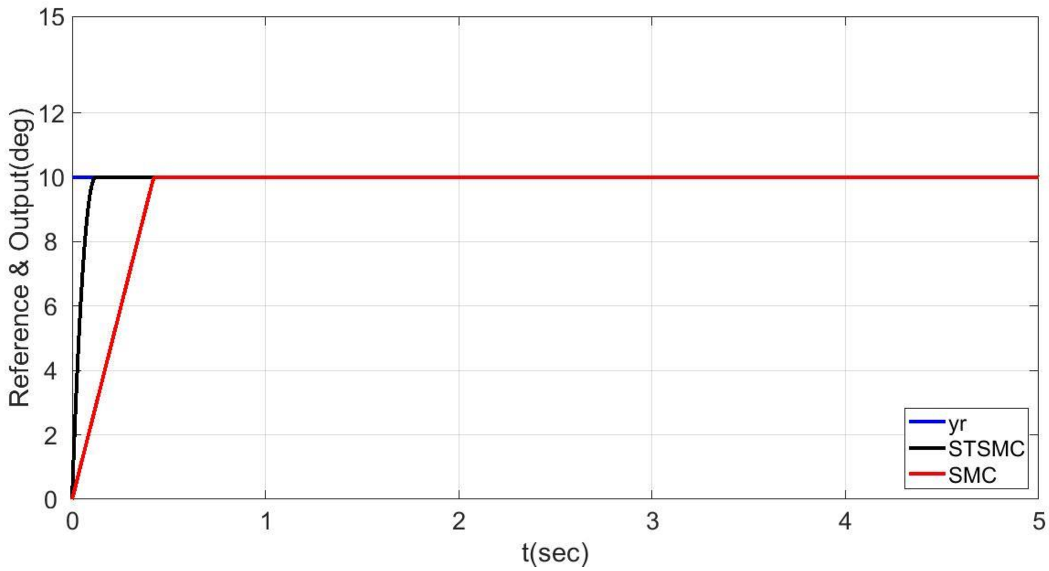

Figure 5.1 The tracking response of SMC and STSMC for single step signal

The simulation results of the SMC and STSMC controllers to this test case for 5 seconds are illustrated in Figures 5.1. It is shown in Figure 5.1 that the control methods follow the reference signal satisfactorily.

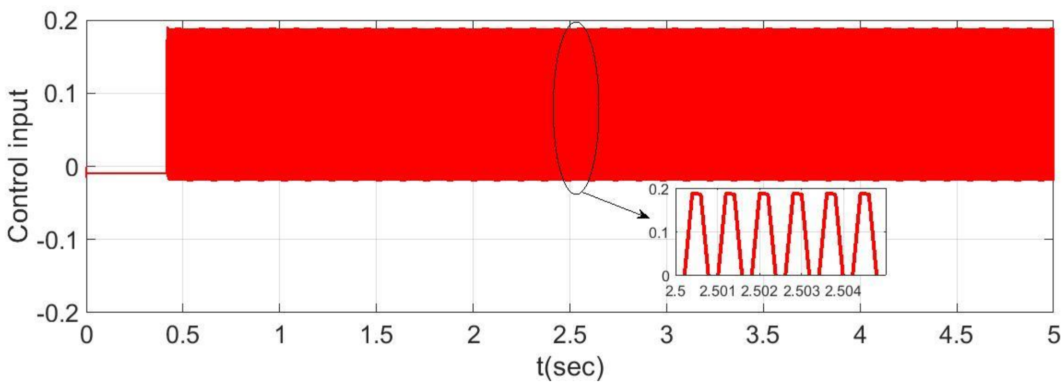

Figure 5.2 control signal of SMC controller for single step signal test

Figure 5.2 shows the control input response of aircraft pitch system using the SMC Controller. So the control signal figure 5.2 shows that the chattering problem of the SMC controller.

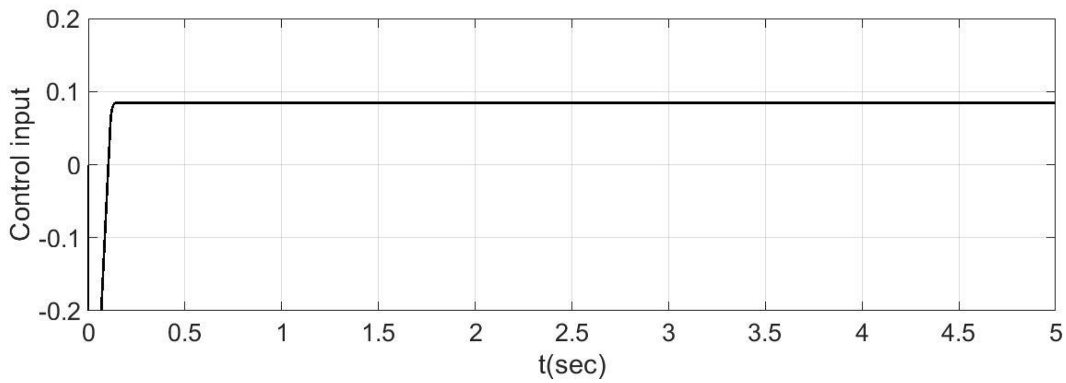

Figure 5.3 Control input signal of STSMC controller for single step signal test

Figure 5.3 illustrates that the control input signal of STSMC controller to track the pitch angle of an aircraft properly without chattering.

As shown in Table 5.3 below, the tracking performance of the SMC control approaches is expressed in terms of IAEU and transient response characteristics, including settling time, Overshoot, rise time, and peak time.

Table 5.3 Tracking performance specifications for single step signal

Tracking controller	Performance characteristics				
	M_p	t_p	t_r	t_s	*IAEU*
STSMC	0.0963	0.1498	0.0762	0.0933	4.08202
SMC	0	0.4324	0.3372	0.4007	4.08613

Table 5.3 which summarizes the step reference performance characteristics of the SMC and STSMC controller. Even though the SMC controller have better performance in overshoot, the STSMC controller reduce the settling time, rise time and peak time by 76.72%, 77.40% and 65.35% respectively. As shown in figure 5.5 STSMC controller eliminate the chattering problem of SMC.

The graphical comparison of the transient performance traits of both controllers for a single step is shown in Figure 5.4. The graph shows that the STSMC controller outperforms the SMC in terms of tracking performance.

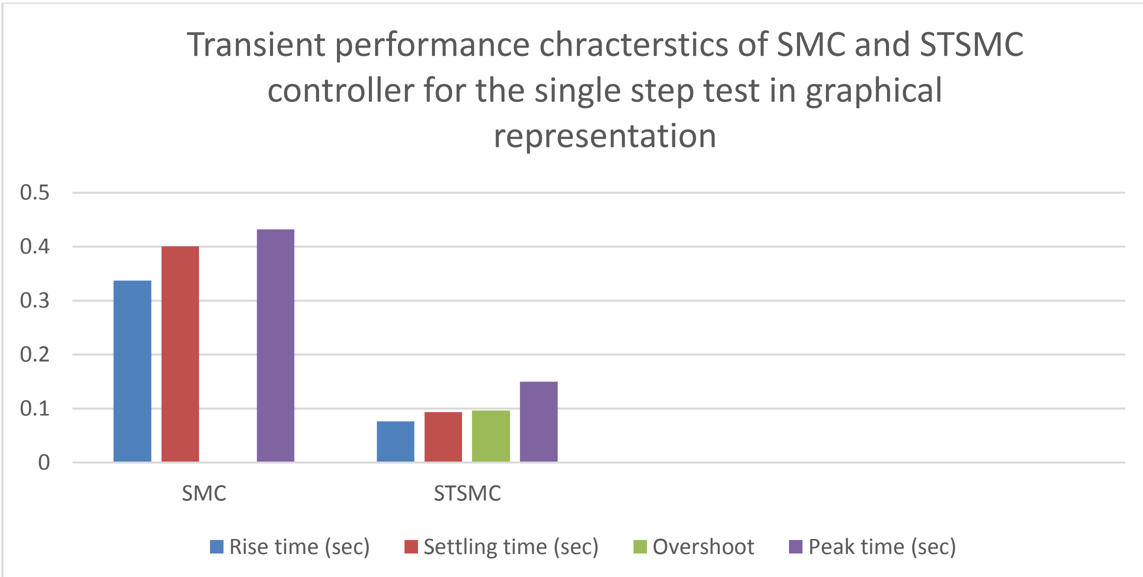

Figure 5.4 Graphical representation of SMC and STSMC controllers for the single step test case tracking performance based on transient performance characteristics

Figure 5.5 depicts the tracking error, which is the difference between the actual output and the desired references.

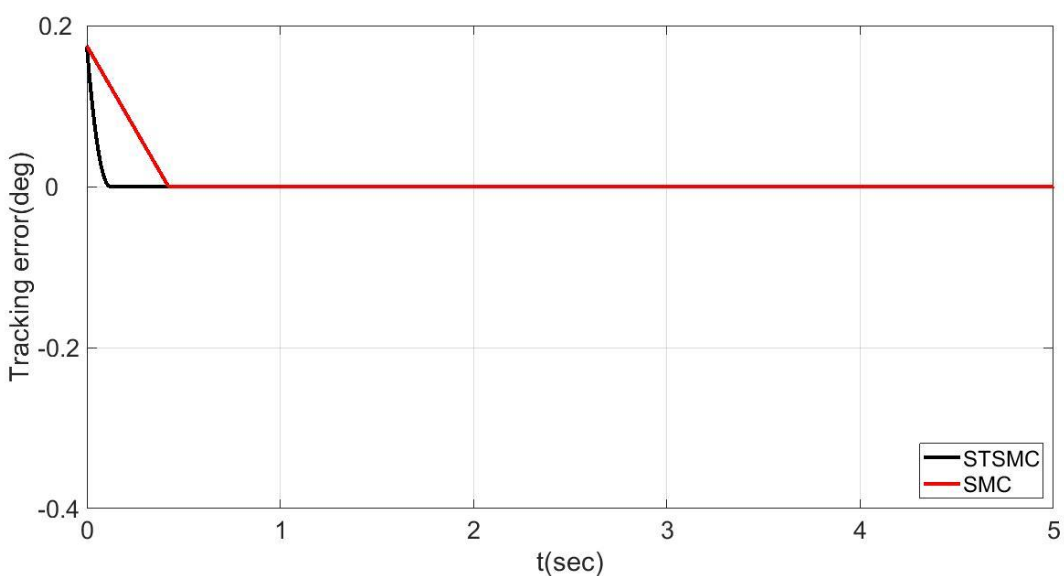

Figure 5.5 Tracking errors for single step signal test case

From Figure 5.5 above, the tracking error converges to zero and remains close to zero for both control strategies. However the proposed STSMC controller's tracking error drops to zero faster than that of the SMC controller.

5.3.1.2 Multiple Step Signals

Several different reference pitch angles are used to run the simulation results. In this case the tracking response is tested when the pitch reference angle is increased from 10^0 to 12^0 (up) initially, then decreased from12^0 to 10^0 (down) at time of 2.5 sec and decreased from 10^0 to 8^0 (down) at time of 5 sec and finally increased from 8^0 to 10^0 (up) at time 7.5 sec. The simulation results of the STSMC and SMC controllers for this scenario over a time period of 10 seconds are shown in Figures 5.6. Both techniques' control parameters are in line with single step signal tracking. According to the tracking answers below, both controllers can trace the reference signal sent to them adequately; however, the SMC has a slower tracking rate than the STSMC, as can be seen in Figure 5.8.

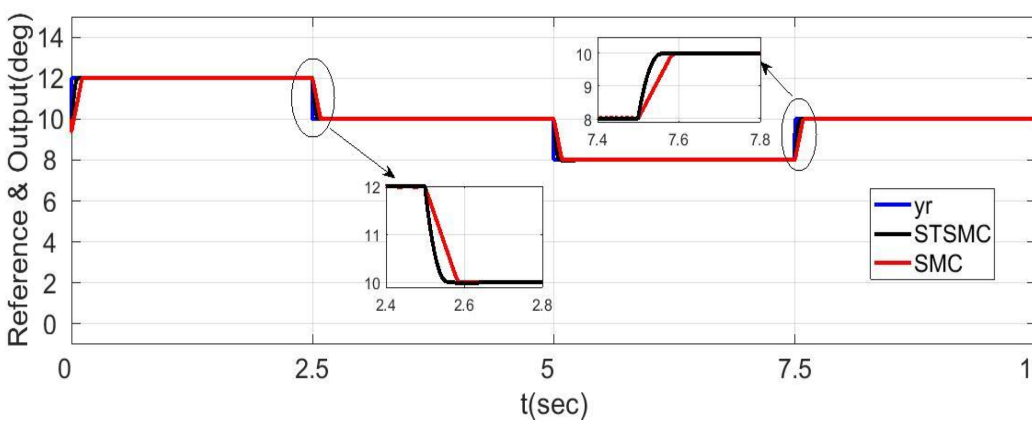

Figure 5.6 The tracking response of SMC and STSMC for multiple step signals

Figure 5.7 shows that the control signals for SMC, so it indicates the chattering problem of SMC controller control signals.

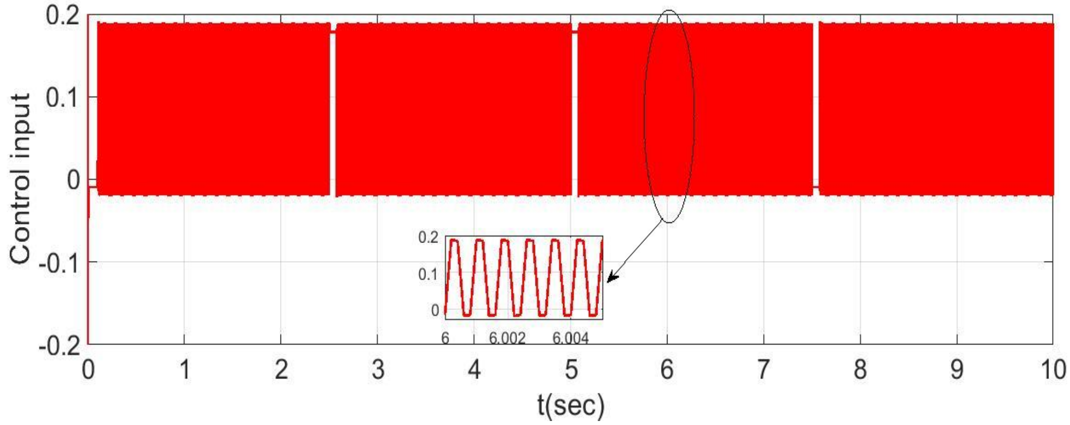

Figure 5.7 Control signal of SMC controller for multiple step signal test

Figure 5.8 shows that the control signal of STSMC as it shown the chattering problem of the SMC controller is solved and to track the reference pitch angle the control effort is fluctuating.

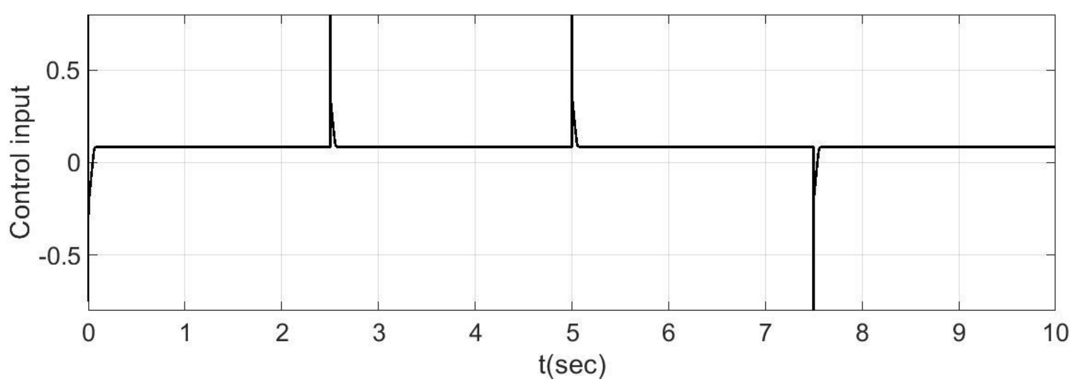

Figure 5.8 Control input signal of STSMC controller for multiple step signal test

Figure 5.9 illustrates how the tracking error of both control techniques, which was nearly zero prior to the modification of the reference signals, re-converges to zero after a brief transience. The zoom portions show, however, that the tracking error of the proposed controller re-converges to zero more quickly than that of the SMC controller. The zoom portions also showed that the suggested STSMC controller has a faster tracking performance because STSMC error changes more quickly than SMC error does.

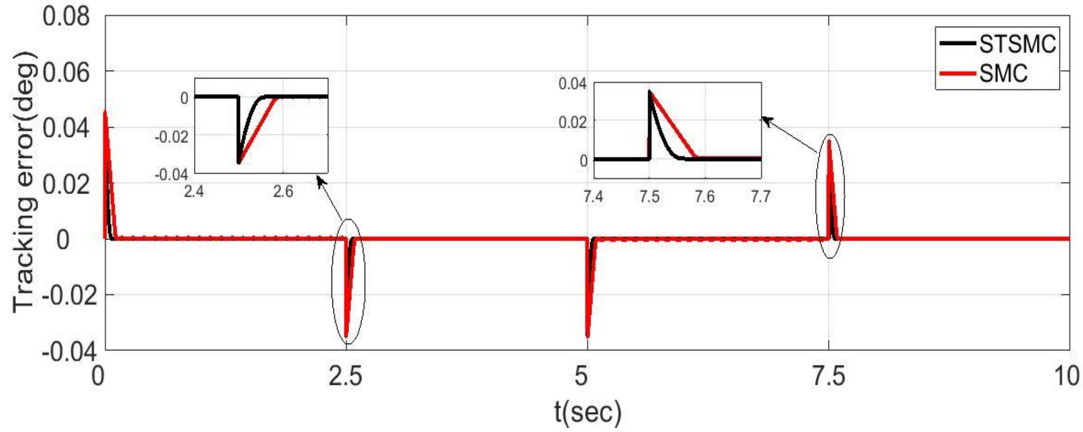

Figure 5.9 Tracking error of both controllers for multiple step signal

5.3.1.3 Ramp Signal

The simulation results are done with a variety of reference pitch angles using ramp signal. In this case the tracking response is tested when the pitch reference angle is $10^0 * \frac{t}{3}$ initially then, it changed to 10^0 and finally it changed to $10^0 * (\frac{-t}{3} + 3)$. The simulation results of the STSMC and SMC controllers for this scenario over a time period of 9 seconds are shown in Figures 5.10. Both techniques' control parameters are in line with single step signal tracking. According to the tracking answers below, both controllers can trace the reference signal sent to them adequately; however, the SMC has a slower tracking rate than the STSMC, as can be seen in Figure 5.12.

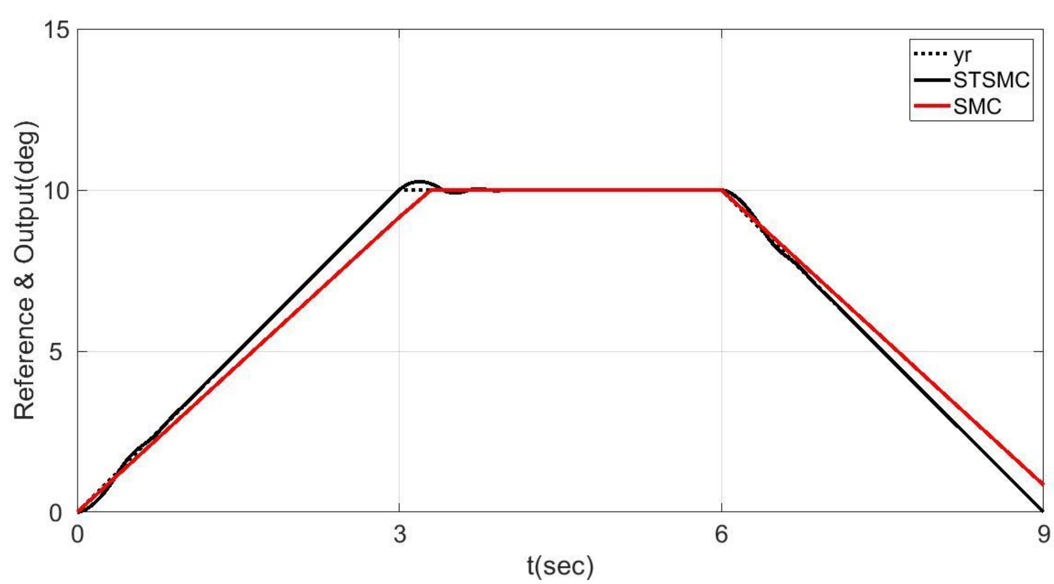

Figure 5.10 The tracking response of SMC and STSMC for ramp signals

Figure 5.11 shows that the control signals for SMC, so it indicates the chattering problem of SMC controller control signals.

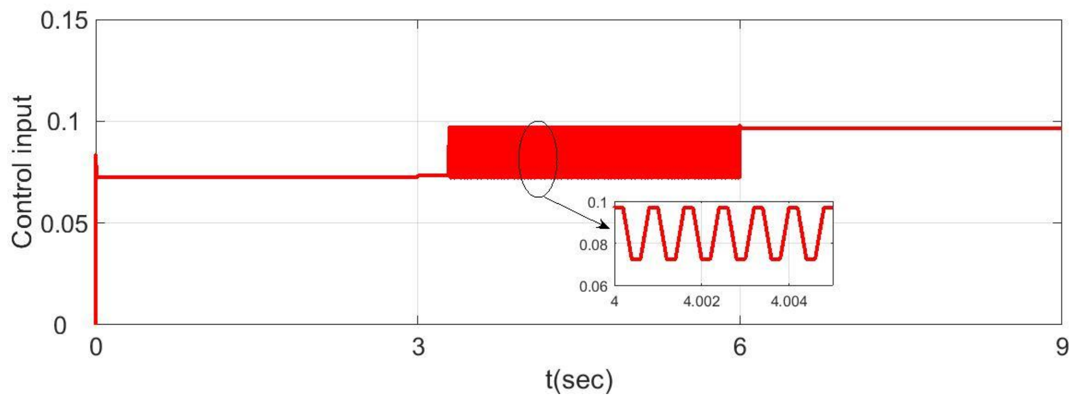

Figure 5.11 Control signal of SMC controller for ramp signal test

Figure 5.12 shows that the control signal of STSMC as it shown the chattering problem of the SMC controller is solved and to track the reference pitch angle the control effort is fluctuating.

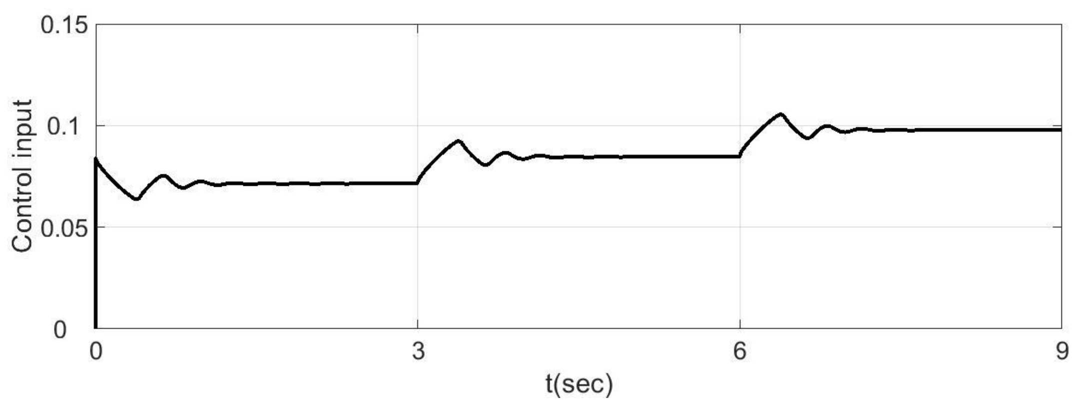

Figure 5.12 Control input signal of STSMC controller for ramp signal test

Figure 5.13 illustrates how the tracking error of both control techniques, which was nearly zero prior to the modification of the reference signals, re-converges to zero after a brief transience. The zoom portions show, however, that the tracking error of the proposed controller re-converges to zero but not the SMC controller. The zoom portions also showed that the suggested STSMC controller has a faster tracking performance because STSMC error changes more quickly than SMC error does.

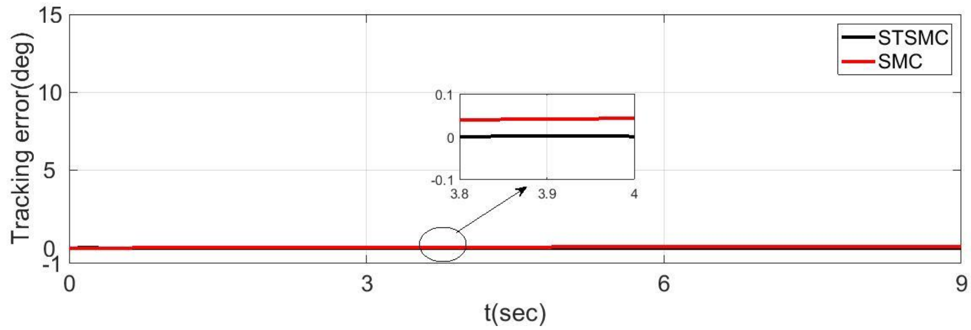

Figure 5.13 Tracking error of both controllers for ramp signal

5.3.2 Robust tracking performance

The aircraft pitch system must be reliable and quick to react in order to prevent a loss of pitch control. The performance robustness of the STSMC and SMC controllers is assessed in this section. In order to verify the system's tracking performance resilience, this thesis study takes into account two different circumstances. The first is parameter variation (change in dynamic pressure), while the second is an outside source causing disturbance.

5.3.2.1 Robustness against parameter variation

This section focuses on the aircraft's dynamic pressure variation, which is a system internal disturbance. Due to variations in air temperature brought on by changes in altitude, the dynamic pressure acting on the aircraft changes. The performance of the controller may suffer as a result of the dynamic pressure variations caused by air temperature. The dynamic pressure parameter fluctuations up to ±10% are taken into consideration in this thesis study. In this part, the robustness of both control techniques is evaluated in the presence of dynamic pressure changes of ±10%.

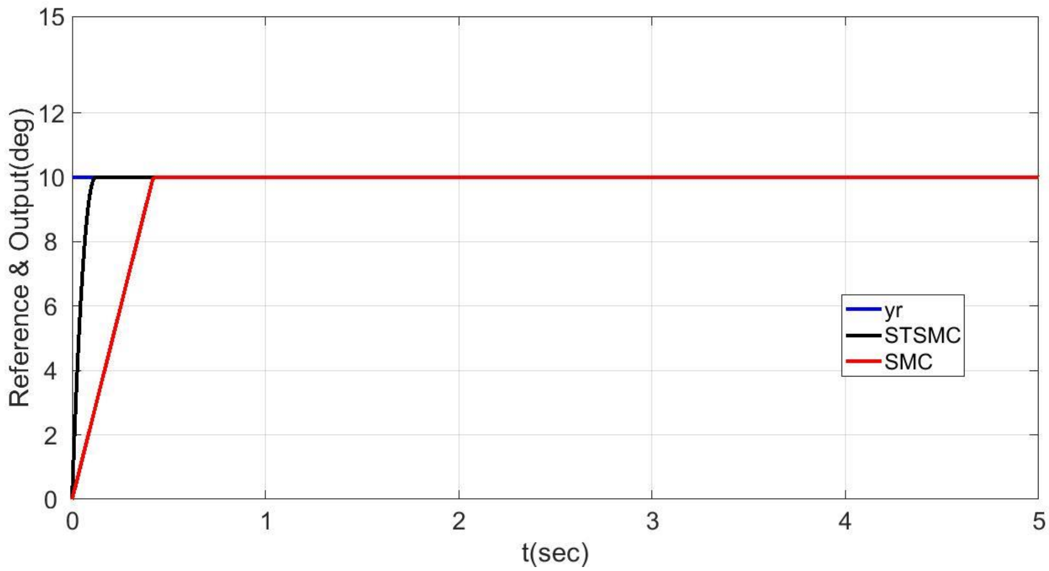

Figure 5.14 Tracking responses with a 10% increment in the dynamic pressure

Table 5.4 Tracking performance specifications for 10% increment in dynamic pressure

Tracking controller	Performance characteristics			
	M_p	t_p	t_r	t_s
STSMC	1.1421	0.1750	0.0877	0.1073
SMC	0	0.5340	0.4192	0.4980

Table 5.4 shows that the performance characteristics of the system pitch response due to increment of dynamic pressure by 10%. The increment of the dynamic pressure by 10% affect the overshoot, peak time, rise time and settling time of the STSMC controller by 3.58%, 0.19%, 0.064% and 0.0275% respectively from the normal condition of the dynamic pressure and the performance SMC controller affect due to the increment of dynamic pressure in rise time and settling time by 0.22% and 0.2% respectively. The proposed STSMC achieves better performance by reducing the peak time by 1.32%, the

rise time by 25.41% and the settling time by 24.4% as compared to the SMC controller. But the overshoot performance of SMC controller is better than STSMC. The result shows that the controller is robust to dynamic pressure increment by 10%.

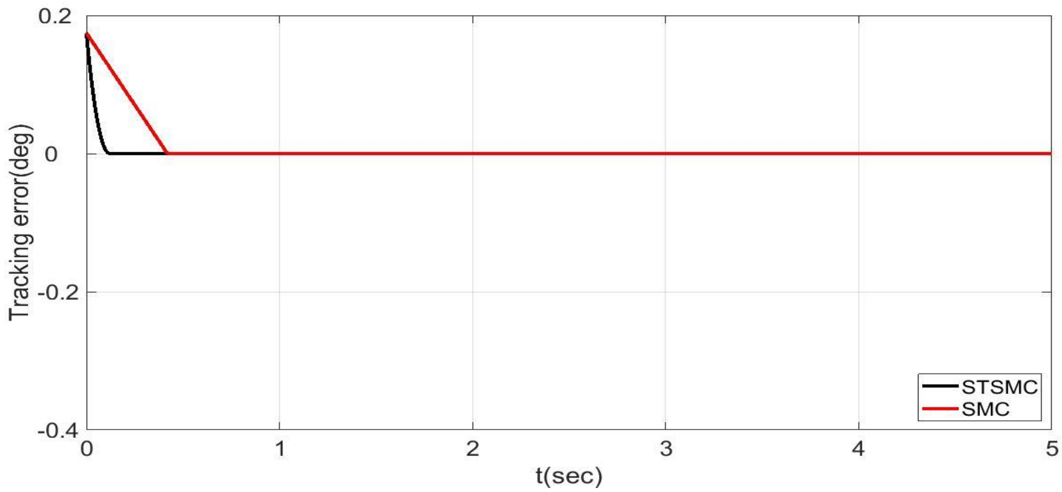

Figure 5.15 Tracking error responses with a 10% increment in the dynamic pressure

The simulation result of the tracking error, presented in Figure 5.15, shows that the tracking error of the proposed controller approaches to zero faster than that of the SMC controller.

Figures 5.16 illustrate the simulation response the STSMC and SMC control strategies for the aircraft when the dynamic pressure decreased by 10%. Both control schemes follow the reference signal nicely in the presence of an internal disturbance. As shown in the figure below. The simulation result shows that the STSMC controller settles to the desired reference signal faster than the SMC controller.

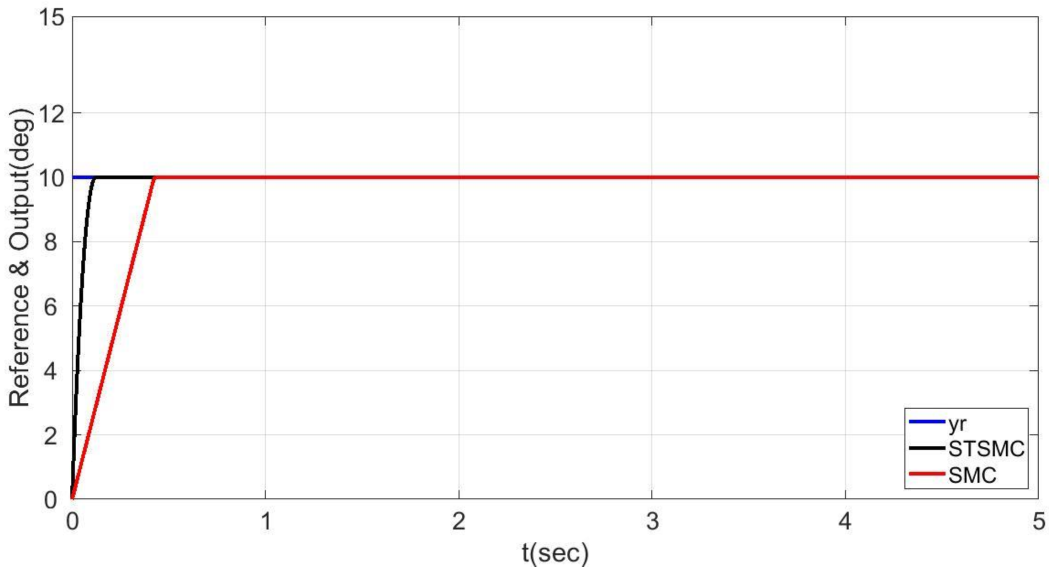

Figure 5.16 Tracking responses with a 10% decrement in the dynamic pressure

Table 5.5 shows that the performance characteristics of the tracking response due the decrement of the dynamic pressure by 10%.

Table 5.5 Tracking performance specifications for 10% decrement in dynamic pressure

Tracking controller	Performance characteristics			
	M_p	t_p	t_r	t_s
STSMC	0.0968	0.1568	0.0767	0.0939
SMC	0	0.4356	0.3396	0.4034

The performance of the SMC controller is impacted by the increment of dynamic pressure in peak time, rise time and settling time increased by 1.66%, 1.6% and 1.61% respectively, and the overshoot, peak time, rise time, and settling time of the STSMC controller increased by 3.58%, 0.19%, 0.064%, and 0.0275%, respectively, from the normal condition of the dynamic pressure.

The proposed STSMC achieves better performance by reducing the peak time by 2.07%, the rise time by 26.5% and the settling time by 24.61% as compared to the SMC controller. But the overshoot performance of SMC controller is better than STSMC. The result shows that the controller is robust to dynamic pressure decrement by 10%.

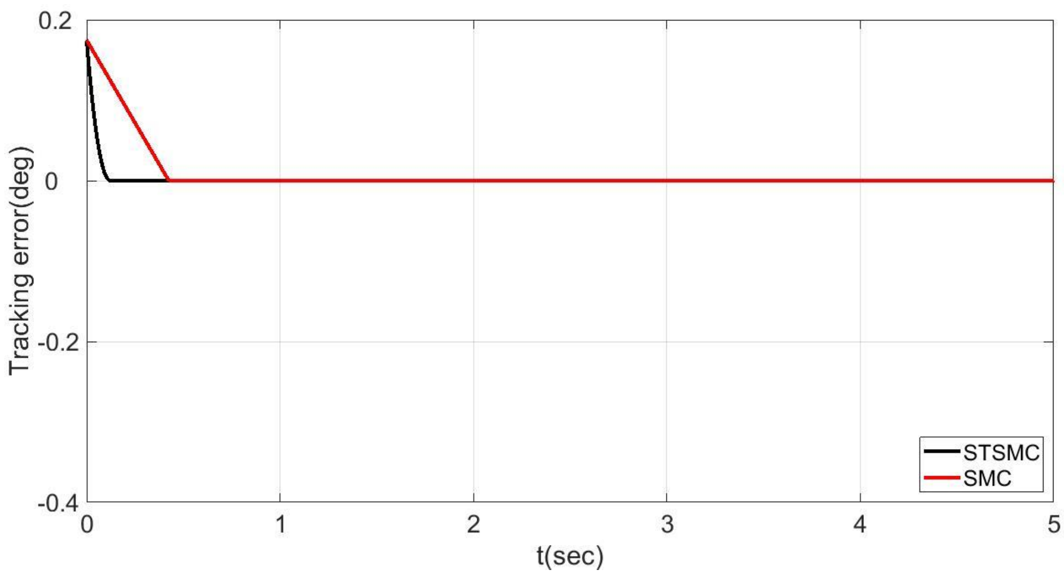

Figure 5.17 Tracking error responses with a 10% decrement in the dynamic pressure

The simulation result of the tracking error, presented in Figure 5.17, shows that the tracking error of the proposed STSMC controller approaches to zero faster than that of the SMC controller.

5.3.2.2 Robustness against external disturbance

In addition to the dynamic pressure, there is an outside disturbance force that affects the airplane. Environmental disturbances, such as a wind-produced external disturbance force, cause the aircraft to move in an unbalanced area. In order to assess the anti-disturbance performance of both control algorithms, a dynamic external disturbance force is applied to the suggested system in this thesis study.

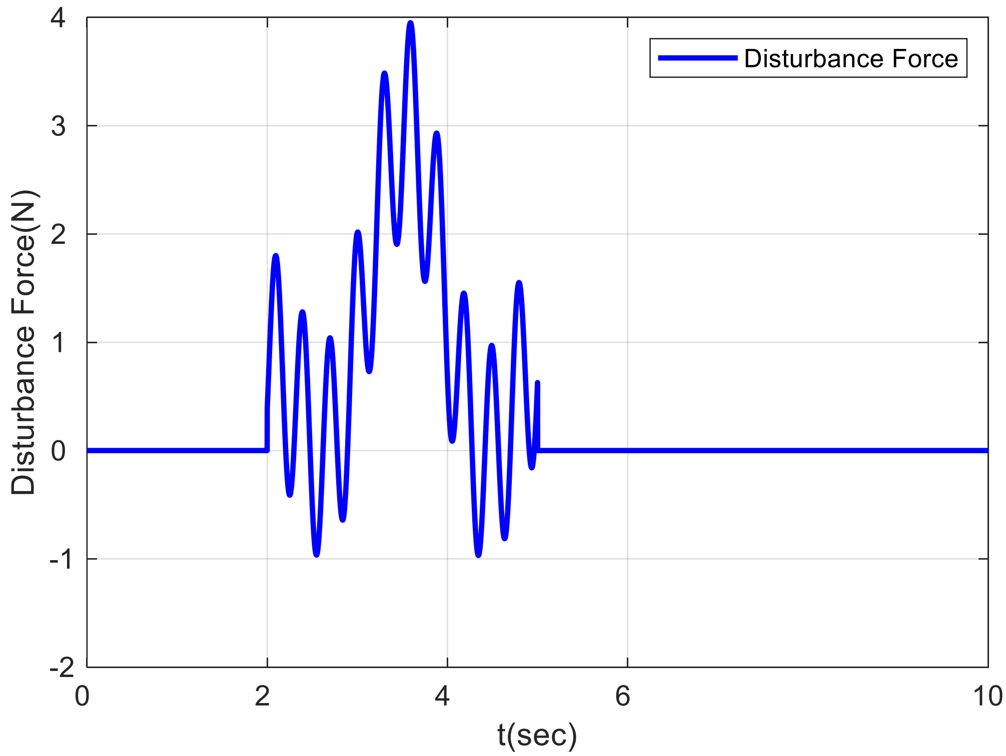

Figure 5.18 Dynamic disturbance force

Figure 5.18 above shows the dynamic disturbance force that was applied to the proposed system at a time of 2 seconds for a length of 3 seconds. Figure 5.19 depicts the system's tracking response to the addition of the dynamic disturbance force mentioned above using both control schemes. Due to the presence of the dynamic disturbance force, Figure 5.19 below shows that both control systems continue to track the given reference with considerable fluctuation. The SMC has a delay tracking compared to the STSMC, as seen in Figure 5.19, although having less fluctuation than the proposed STSMC controller.

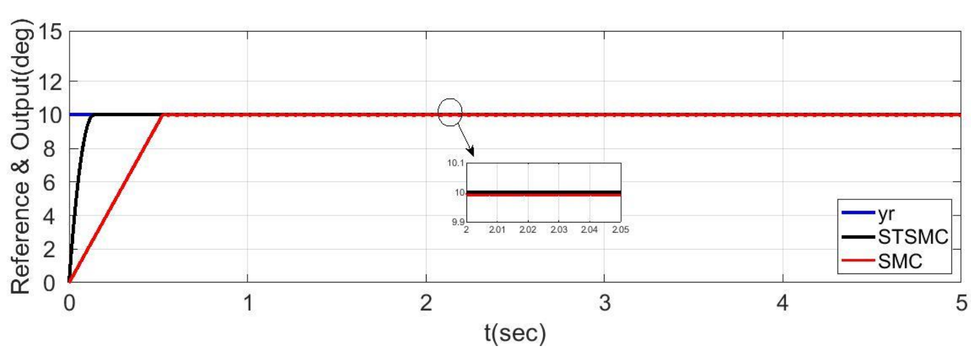

Figure 5.19 Tracking response under the effect of dynamic disturbance force

Table 5.6 displays a quantitative comparison of both control algorithms in the presence of a dynamic disturbance force.

Table 5.6 Performance measures under the existence of a dynamic disturbance force.

Tracking controller	Performance characteristics			
	M_p	t_p	t_r	t_s
STSMC	0.7025	0.1620	0.0785	0.0951
SMC	0.0744	1.0430	0.3558	0.4202

Despite the STSMC's significant overshoot, the other performance metrics, as shown in Table 5.5, have lower values. The proposed STSMC controller achieves better performance by reducing the peak time by 84.5%, the rise time by 77.93% and the settling time by 77.4% as compared to the SMC controller. According to the aforementioned tabular result, the suggested STSMC control method is more resistant to dynamic external disturbance forces than the SMC controller.

Figure 5.20 depicts the tracking error response of both controllers under the existence of dynamic external disturbance force.

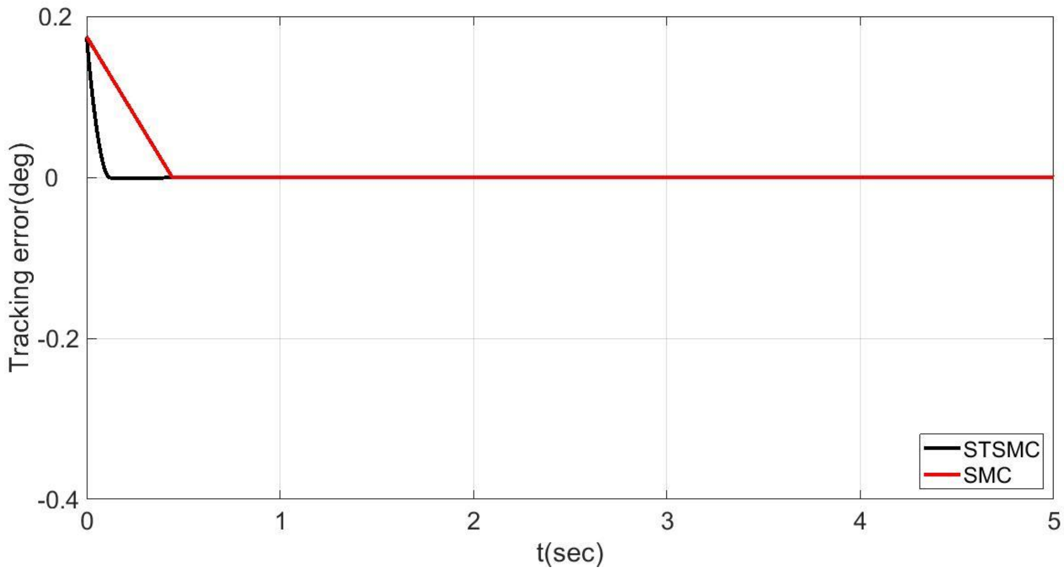

Figure 5.20 Tracking error responses under the effect of dynamic disturbance force

The tracking error graph demonstrates that the STSMC controller's tracking error re-converges to zero more quickly than the SMC controller's tracking error.

5.3.2.3 Robustness against both dynamic pressure variation and wind disturbance

The two sections above confirm that both dynamic pressure changes and outside disturbances have an impact on the proposed system's tracking capability. Therefore, this part analyzes the tracking performance and robustness of the suggested system utilizing the STSMC and SMC control algorithms while both dynamic external disturbance force and dynamic pressure change are present. Here, the dynamic pressure is utilized as it rises 10%.

Figure 5.21 shows the tracking response of both controllers when the dynamic external disturbance force discussed in section 5.3.2.2 and the dynamic pressure is increased by 10% is added to the system.

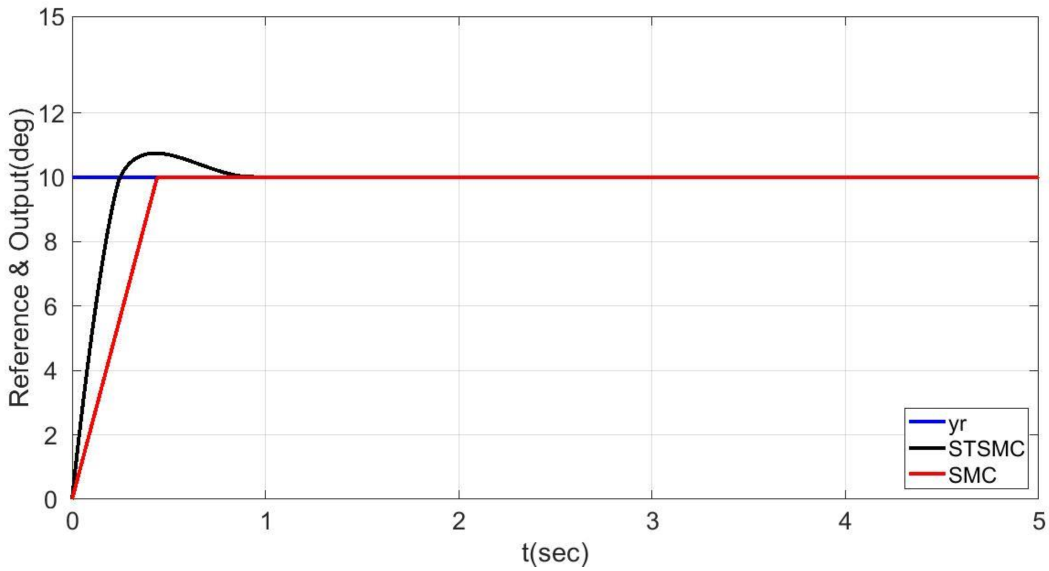

Figure 5.21 Tracking performances of both controllers with the effect of both increment of dynamic pressure by 10% and dynamic disturbance force

The quantitative comparison of both control algorithms under the existence of both increment of dynamic pressure by 10% and a dynamic external disturbance force is shown in Table 5.7.

Table 5.7 Performance measures under the existence of a dynamic disturbance force and dynamic pressure increment by 10%

Tracking controller	Performance characteristics			
	M_p	t_p	t_r	t_s
STSMC	7.4819	0.4314	0.1879	0.6145
SMC	3.4476	5.0000	0.3713	0.4410

The SMC controller has better performance on overshoot and settling time but the STSMC reduce the rise time and the peak time by 49.39% and 91.37% respectively.

The results shown in the above table demonstrate that the suggested control mechanism is more resistant to dynamic external disturbance force and dynamic pressure increment.

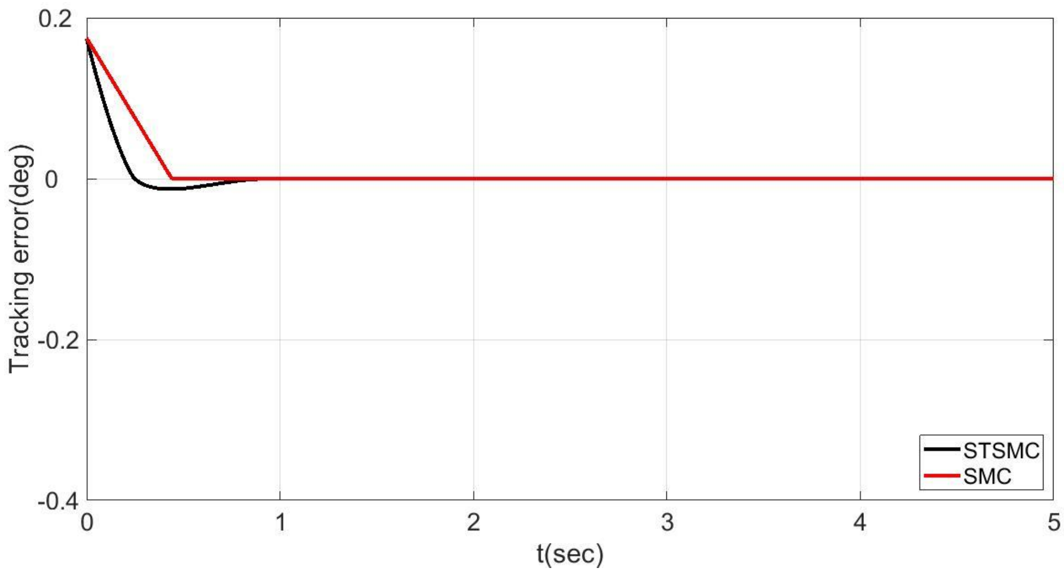

Figure 5.22 Tracking errors of both controllers under the effect of both dynamic pressure increment and dynamic disturbance force

Due to the presence of both dynamic pressure increment and the dynamic external disturbance force, as shown in Figure 5.22 above, the tracking error of both controllers varies. The tracking error of the proposed STSMC controller re-converges close to zero despite fluctuating more than the SMC controller. As a result, the STSMC is resistant to both the dynamic external disturbance force and the dynamic pressure increment.

CHAPTER SIX

CONCLUSION AND RECOMMENDATION

6.1 Conclusion

Since the aircraft system is nonlinear and unstable, this thesis work designs a super twisting sliding mode controller. The aircraft's mathematical model is first derived. The airplane's pitch is then controlled using the longitudinal model of the aircraft. The super twisting control technique is intended to track and manage an aircraft's pitch. The conventional sliding mode controller is used for the comparison with super twisting sliding mode controller. The developed super twisting sliding mode and the conventional sliding mode controller's parameter values are optimized using the particle swarm optimization technique.

The evaluation of both controllers' tracking abilities was done using various references and the robustness of the tracking performance under the influence of dynamic pressure change and external dynamic disturbance force was tested. To compare the tracking performance, the proposed performance index (IAEU) and the transient performance traits overshoot, peak time, settling time, and rise time are used.

The proposed STSMC has lower values of settling time, rise time, peak time, and IAEU value in the case of all references used in this research work, which verifies that the proposed super twisting sliding mode control scheme has better tracking performance ability. This is shown by the tracking capability test using different references, which compares the proposed STSMC to each reference.

To evaluate the robustness against parameter variation tracking performance's resistance to dynamic pressure change is investigated in this thesis work up to ±10% change. The SMC controller wasn't as effective as the intended controller.

This thesis work additionally employs a dynamic external disturbance force to examine the tracking performance resilience of both controllers under the influence of this disturbance. The SMC has greater fluctuation in its tracking performance resilience against this disturbance force than the STSMC controller. Compared to the SMC controller, the proposed STSMC control settles to the required reference more quickly.

The obtained simulation results demonstrate that the STSMC technique outperforms the SMC under normal conditions by reducing the settling time, rise time, and peak time by, respectively, 76.72%, 77.40%, and 65.35%. Peak, rising, and settling periods in the 10% increment of dynamic pressure are, respectively, 0.1750 seconds, 0.0877 seconds, and 0.1073 seconds when using the suggested STSMC control strategy. When compared to the SMC, the times are minimal. During the external disturbance force rejection test, the STSMC outputs 0.1620sec, 0.0785sec, and 0.0951sec of peak, rising, and settling times. For the tracking performance robustness against both dynamic pressure fluctuations and external disturbance force, the STSMC gives 0.4314sec of peak time, 0.1879sec of rising time, and 0.6145sec of settling time, which are all minimal compared to the SMC.

The STSMC controller generally offers higher tracking performance and has a better ability to manage the effects of dynamic pressure changes and external disturbance force, according to the overall simulation results of this research effort.

6.2 Recommendation

Under the influence of parameter uncertainty from dynamic pressure variation and rapid external disturbance force, the aircraft pitch system must be stable and capable of tracking any reference signal. So, this research work may be made even better by utilizing an adaptive super twisting sliding mode control method, which can offer the optimum response when there are a variety of dynamic pressure variations and unexpected disturbance forces.

Future researches are anticipated to use the STSMCs on a full nonlinear state model into a cascade structure to establish a global stability.

Research fund Acknowledgment

This research thesis was funded by Adama Science and Technology University under the grant number ASTU/SM-R/536/22, Adama, Ethiopia.

REFERENCES

Ahmad, M., Hussain, Z. L., Irtiza, S., Shah, A., & Shams, T. A. (2021). *applied sciences Estimation of Stability Parameters for Wide Body Aircraft Using Computational Techniques*.

Arrosida, H., & Echsony, M. E. (2017). *Aircraft Pitch Control Design Using Observer-State Feedback Control*. *2*(4), 263–272.

Bouadi, H., Control, F., Design, L., & Auto-, A. T. T. (2014). *Contribution to Flight Control Law Design and Aircraft Trajectory Tracking To cite this version : HAL Id : tel-00974871*.

Chen, J., Omidvar, M. N., Azad, M., & Yao, X. (2017). Knowledge-based particle swarm optimization for PID controller tuning. *2017 IEEE Congress on Evolutionary Computation, CEC 2017 - Proceedings*, 1819–1826. https://doi.org/10.1109/CEC.2017.7969522

Chrif, L., Kada, Z. M., & Mohamed, T. (2015). *Flight-Path Tracking Control of an Aircraft Using Backstepping Controller*. *15*(2), 270–276. https://doi.org/10.11591/telkomnika.v15i2.8101

Cunjia, L., Wen, H., (2016). *Disturbance rejection flight control for small fixed-wing unmanned aerial vehicles American Institute of Aeronautics and Astronautics Disturbance rejection flight control for small fixed-wing unmanned aerial vehicles*. 0–23.

Duncan, S. (2016). *Aerodynamics of Flight*. *Cl*. 1–12.

Erbatur, K., Kaynak, O., & Member, S. (2001). *Use of Adaptive Fuzzy Systems in Parameter Tuning of Sliding-Mode Controllers*. *6*(4), 474–482.

Gad, A. G. (2022). Particle Swarm Optimization Algorithm and Its Applications: A Systematic Review. In *Archives of Computational Methods in Engineering* (Issue 0123456789). Springer Netherlands. https://doi.org/10.1007/s11831-021-09694-4

Hamid, T., & Babar, M. Z. (2019). *Pitch Attitude Control for an Aircraft using Linear Quadratic Integral Control Strategy*.

Ibrahim, E. (2013). *City , University of London Institutional Repository Mathematical Modelling , Flight Control System*.

J.Jebakumar, K.Mishra, & B.MISHRA. (2014). Controller Selection and Sensitivity Check on the Basic of Performance Index Calculation. *International Journal of Electrical, Electronics and Data Communication*, *2*(1), 91–93.

Johari, A., Yakub, F., Ariff, H., Rasid, Z. A., & Sarip, S. (2018). *Improvement of Pitch Motion Control of an Aircraft Systems Improvement of Pitch Motion Control of an Aircraft Systems*. *December 2019*. https://doi.org/10.12928/telkomnika.v16i5.7434

John S. (2016). Pilot Hand Book of Aeronautical knowledge

Khalid, A., Zeb, K., Haider, A., & Ieee, S. (n.d.). Conventional PID , Adaptive PID , and Sliding Mode controllers design for Aircraft Pitch Control. *2019 International Conference on Engineering and Emerging Technologies (ICEET)*, 1–6.

Lee, S., Lee, B., & You, S. L. B. L. S. (2018). *Sliding Mode Control with Super-Twisting Algorithm for Surge Oscillation of Mooring Vessel System 슈퍼트위스팅 슬라이딩모드를 이용한 선박계류시스템의 동적제어*. *24*(7), 953–959.

Li, X.-L., Serra, R., & Olivier, J. (2019). Effects of Particle Swarm Optimization Algorithm Parameters for Structural Dynamic Monitoring of Cantilever Beam. *Surveillance, Vishno and AVE Conferences*, 1–7. https://www.semanticscholar.org/paper/Effects-of-Particle-Swarm-Optimization-Algorithm-of-Xiao-lin-Serra/0d7a6c8cd6467e6182299e9ad7bcf567d715b054#paper-header

Li, Y., & Peng, C. (2021). *Super-Twisting Sliding Mode Control Law Design for Attitude Tracking Task of a Spacecraft via Reaction Wheels*. *2021*.

Nakisa, B., Nazri, M. Z. A., Rastgoo, M. N., & Abdullah, S. (2014). A survey: Particle swarm optimization based algorithms to solve premature convergence problem. *Journal of Computer Science*, *10*(10), 1758–1765. https://doi.org/10.3844/jcssp.2014.1758.1765

N. Wahid and N. Hassan, "Self-Tuning Fuzzy PID Controller Design for Aircraft Pitch

Control," *2012 Third International Conference on Intelligent Systems Modelling and Simulation*, Kota Kinabalu, Malaysia, 2012, pp. 19-24, doi: 10.1109/ISMS.2012.27.

Particle Swarm optimization Contents. (n.d.).

Patel, S. H. (2007). *Introduction to QFT*. *April*.

Păucă, O., & Mirea, L. (2017). *Comparative Study on Pitch Angle Control of an Aircraft Using Neural Networks*. 340–345.

Radhakrishnan, C. (2020). *Performance Comparison for Fuzzy based Aircraft Pitch using Various Control Methods*. 428–433.

Radhakrishnan, C., & Swarup, A. (2020). *Improved Aircraft Performance using Simple Pitch Control*. 295–299.

Rahul B and Dharani J, "Genetic Algorithm tuned PID Controller for Aircraft Pitch Control," 2019 nternational Journal for Research in Engineering Application & Management (IJREAM) DOI : 10.18231/2454-9150.2018.1324

Shaji, J. (2015). *Pitch Control of Flight System using Dynamic Inversion and PID Controller*. *4*(07), 604–608.

Sivaramakrishna, G., & Santhi, R. V. (2017). *Design of Adaptive Sliding Mode Control with Fuzzy Controller and PID Tuning for Uncertain Systems*. 213–217.

Sudha, G., & Deepa, S. N. (2016). *Optimization for PID Control Parameters on Pitch Control of Aircraft Dynamics Based on Tuning Methods*. *350*(1), 343–350.

Thanu, T. T. (2016). *ODU Digital Commons Nonlinear Flight Control Design Using Backstepping Methodology*. https://doi.org/10.25777/04v9-gf94

Training, F. O. R., & Only, P. (2017). *Basic aerodynamics*. *1*.

Wahid, N., Rahmat, M. F., & Jusoff, K. (2010). *Comparative Assessment using LQR and Fuzzy Logic Controller for a Pitch Control System*. *January 2015*.

APPENDICES

APPENDIX A

A.1 MATLAB code for open loop response of the nonlinear model

```
function openloop
global rho Vt Sc Cd Cl0 Cldh Ct Clq Cm0 Cmdh Cmq T g m Iyy
Cd= 0.0393; Cl0= 0.12; Cldh= 0.356; Clq= 5.13;
Cm0= 0.121; Cmdh= -1.43; Cmq= -20.7;
Sc= 5500; Ct= 27.3; Vt= 871; rho= 222.8;
Iyy= 3.31e+7; T= 54750; m= 636636; g= 32.17;
t= 0; h= 0.0002; loop= 45000;
x= [0 0 0.1 0 0 0 0]';
buf= [t x' 1];
for i=1:loop
   u=1;
    x= RK4(@Aircraft, t, x, u, h);
   t= t+h;
   y= x(6);
   buf= [buf;t x' u];
end
t=buf(:,1); y=buf(:,2);
plot(t,y,'k','linewidth',2);
xlabel('t(sec)'),ylabel('Output(deg)')
title('open loop resopnse of the system')
function xdot= Aircraft(t,x,u)
global rho Vt Sc Cd Cl0 Cldh Ct Clq Cm0 Cmdh Cmq T g m Iyy
D= 0.5*rho*Vt^2*Sc*Cd;
L= 0.5*rho*Vt^2*Sc*(Cl0+Cldh*u+0.5*Ct/Vt*Clq*x(7));
M= 0.5*rho*Vt^2*Sc*(Cm0+Cmdh*u+0.5*Ct/Vt*Cmq*x(7));
```

```
xdot= zeros(7,1);
xdot(1)= x(3)*cos(x(5));
xdot(2)= -x(3)*sin(x(5));
xdot(3)= (-D+T*cos(x(4))-m*g*sin(x(5)))/m;
xdot(4)= x(7)+(-L-T*sin(x(4))+m*g*cos(x(5)))/(m*x(3));
xdot(5)= (T*sin(x(4))+L-m*g*cos(x(5)))/(m*x(3));
xdot(6)= x(7);
xdot(7)= M/Iyy
```

APPENDIX B

B.1 MATLAB code for STSMC control system

```
function SimSTSMC_Step_UP
global rho Vt Sc Cd Cl0 Cldh Ct Clq Cm0 Cmdh Cmq T g m Iyy
Cd= 0.0393; Cl0= 0.12; Cldh= 0.356; Clq= 5.13;
Cm0= 0.121; Cmdh= -1.43; Cmq= -20.7;
Sc= 5500; Ct= 27.3; Vt= 871;
 rho= 222.8;
Iyy= 3.31e+7;
T= 54750;
 m= 636636;
g= 32.17;
k1=234.9333;k2=0.0144;k3=0.0535;
t= 0; h= 0.0002; loop= 25000;
x= [0 0 0.1 0 0 0 0]'; y= x(6); % Initial states
yr= deg2rad(10); % Reference input in degree
dyr= 0; ddyr= 0; % Reference input
v= 0; ww= 0; yy= 0; ee= 0; % Other initial values
e=yr-y;
buf= [t yr y 0 e];
```

```
for i=1:loop
   e= yr-y;
   de= (e-ee)/h; ee= e;
   s= k1*e+de;
%    w= -k3*sign(s);
   w= -k3*tanh(s/0.1);
   v= v+0.5*h*(w+ww); ww= w;
   dy= (y-yy)/h; yy= y;
   u1= 2*Iyy*(ddyr+k1*dyr-k1*dy)/(rho*Vt^2*Sc*Cmdh);
   u2= -Ct*Cmq*x(7)/(2*Vt^2*Cmdh)-Cm0/Cmdh-k2*sqrt(abs(s))*tanh(s/0.1)+v;
   u= u1+u2;
   % Calls the aircraft system
   x= RK4(@Aircraft, t, x, u, h);
   t= t+h;
   y= x(6);
   buf= [buf;t yr y u e];
end
w= 5;
ae= abs(yr-buf(:,3))+w*abs(buf(:,4));
J= 0.5*h*(ae(1)+2*sum(ae(2:end-1))+ae(end))
buf(:,2:3)= rad2deg(buf(:,2:3));
save 'IAEU_Step_UP' 'buf'
gh= plot(buf(:,1),buf(:,2),'r',buf(:,1),buf(:,3),'k','linewidth',2);
set(gh(1),'linewidth',1);
legend('yr','y')
xlabel('t(sec)'),ylabel('Reference & Output(deg)')
axis([0 h*loop 0 15])
grid on;
function xdot= Aircraft(t,x,u)
global rho Vt Sc Cd Cl0 Cldh Ct Clq Cm0 Cmdh Cmq T g m Iyy
D= 0.5*rho*Vt^2*Sc*Cd;
```

```
L= 0.5*rho*Vt^2*Sc*(Cl0+Cldh*u+0.5*Ct/Vt*Clq*x(7));
M= 0.5*rho*Vt^2*Sc*(Cm0+Cmdh*u+0.5*Ct/Vt*Cmq*x(7));
xdot= zeros(7,1);
xdot(1)= x(3)*cos(x(5));
xdot(2)= -x(3)*sin(x(5));
xdot(3)= (-D+T*cos(x(4))-m*g*sin(x(5)))/m;
xdot(4)= x(7)+(-L-T*sin(x(4))+m*g*cos(x(5)))/(m*x(3));
xdot(5)= (T*sin(x(4))+L-m*g*cos(x(5)))/(m*x(3));
xdot(6)= x(7);
xdot(7)= M/Iyy;
```

B.2 MATLAB code for the PSO algorithm

```
function TuneSTSMC
options = optimoptions('particleswarm');
options.PlotFcn= 'pswplotbestf';
options.InertiaRange= [0.4,0.9];
options.SelfAdjustmentWeight=2;
options.SocialAdjustmentWeight=2;
options.MaxIterations= 30;
options.SwarmSize= 20;
nvar= 3;
LB= [0.0001 0.0001 0.0001];
UB= [300 0.1 0.1];
[x,fval]= particleswarm(@EvalObj,nvar,LB,UB,options)
```